EFFECTS OF WILDTYPE AND MUTANT FORMS OF ATRIAL NATRIURETIC PEPTIDE ON L-TYPE Ca^{2+} CURRENT IN MOUSE ATRIAL MYOCYTES

by

Sarah L. MacLeod

Submitted in partial fulfillment of the requirements
for the degree of Master of Science

at

Dalhousie University
Halifax, Nova Scotia
March 2014

This thesis is dedicated to the friendship and memory of

Alex Taylor, my favourite science geek.

TABLE OF CONTENTS

LIST OF TABLES

LIST OF FIGURES

ABSTRACT

Atrial natriuretic peptide (ANP) is a hormone with numerous effects in the cardiovascular system, including ion channel physiology. Genetic mapping of a family with hereditary atrial fibrillation (AF) revealed a mutation that produced a mutant ANP (mANP). We used patch-clamping and cAMP assays to investigate the electrophysiological effects of ANP and mANP in mouse atrial myocytes. ANP and mANP had no effects in basal conditions. In the presence of the β-adrenergic receptor agonist isoproterenol (ISO), ANP increased $I_{Ca,L}$ density, maximal conductance (G_{max}) and hyperpolarized the $V_{1/2}$ of channel activation ($V_{1/2(act)}$). ISO and ANP also increased cAMP production. In contrast, ISO+mANP decreased $I_{Ca,L}$ density, G_{max} and depolarized the $V_{1/2(act)}$ and also decreased cAMP production. ANP's effects on $I_{Ca,L}$ were maintained in NPR-$C^{-/-}$ mice, but absent following NPR-A blockade. mANP effects on $I_{Ca,L}$ were lost in NPR-$C^{-/-}$ mice. These opposing effects of ANP and mANP may explain how mANP causes AF.

LIST OF ABBREVIATIONS USED

β-AR	β-adrenergic receptor
AC	adenylyl cyclase
ACE	angiotensin converting enzyme
AF	atrial fibrillation
Ang II	angiotension II
ANP	atrial natriuretic peptide
AP	action potential
APD_{50}	action potential duration at 50% repolarization
APD_{70}	action potential duration at 70% repolarization
APD_{90}	action potential duration at 90% repolarization
ATP	adenosine triphosphate
AVN	atrioventricular node
BNP	brain type natriuretic peptide
BP	blood pressure
cAMP	cyclic adenosine monophosphate
cGMP	cyclic guanosine monophosphate
CNP	C-type natriuretic peptide
DAG	diacylglycerol
DD-H2O	double distilled water
ERP	effective refractory period
GC	guanylyl cyclase
G_i	inhibitory G protein

G_{max}	maximum current conductance
G_s	stimulatory G protein
GTP	guanosine triphosphate
I_{Ca}	inward calcium current
$I_{Ca,L}$	L-type calcium current
I_f	hyperpolarization activated current
I_{K1}	inwardly rectifying potassium current
I_K	potassium currents
I_{KATP}	ATP-sensitive potassium current
I_{Kr}	rapidly activating outwardly rectifying potassium current
I_{Ks}	slow activating outwardly rectifying potassium current
I_{Kur}	outward delayed rectifier potassium current
I_{Na}	inward sodium currents
I_{to}	transient outward potassium current
IP3	inositol triphosphate
ISO	isoproterenol
IV	current-voltage relationship
k	activation curve slope constant
KHD	kinase homology domain
LTCC	L-type calcium channel
mANP	mutant form of ANP
NP	natriuretic peptide
NPR	natriuretic peptide receptor

NPR-A	natriuretic peptide receptor - A
NPR-B	natriuretic peptide receptor - B
NPR-C	natriuretic peptide receptor - C
PDE	phosphodiesterase
PKA	protein kinase A
PKC	protein kinase C
PKG	protein kinase G
PLCβ	phospholipase C, β isoform
RAAS	renin-angiotensin-aldosterone system
RMP	resting membrane potential
SAN	sinoatrial node
SNP	single-nucleotide polymorphism
$V_{1/2}$	voltage required for 50% channel activation
V_{max}	maximum rate of depolarization
WT	wild type

ACKNOWLEDGEMENT

"True education does not consist merely in the

acquiring of a few facts of science…,

but in the development of character."

D.O.M.

I would like to give my most sincerest thanks to Dr. Robert Rose for the amazing opportunity and environment to acquire a high level scientific education and for indispensable character development. These are skills that I will take with me throughout my life.

I would also like to thank my supervisory committee, consisting of Dr. Susan Howlett and Dr. Xianping Dong, for their guidance and attendance over the past 2 years. Thanks also to Dr. Stacy O'Blenes for acting as a third reader and his contributions to my final thesis, and to Dr. Liz Cowley, Dr. Nik Morgunov and Jennifer Graves for all of their support and hard work.

Thank you to Randi Parks, Dr. Denis Dupré, Jaime Wertman and Jessica MacLean for their very much appreciated help with the cAMP assays done for this study.

In addition, my never-ending gratitude goes to my friends, in and out of the lab, and family for their love and encouragement as I followed my scientific curiosity. I cannot put into words my appreciation for everyone who has helped me throughout this degree.

S.

CHAPTER 1: INTRODUCTION

1.1 Overview

Atrial fibrillation (AF), the most common sustained cardiac arrhythmia (Dobrev & Nattel, 2010), is characterized by rapid and irregular activation of the atria (up to 400-600 beats/min in humans) and is a major cause of morbidity and mortality (Benjamin *et al*., 1998; Benjamin *et al*., 2009). Natriuretic peptides (NPs), which constitute a family of cardioprotective hormones, have been directly implicated in the pathogenesis of AF (Abraham *et al*., 2010; Hodgson-Zingman *et al,* 2000*)*. NPs, including atrial (ANP), B-type (BNP) and C-type (CNP) NP, are best known for their important role in the regulation of blood pressure (BP) and blood volume, whereas the electrophysiological effects of NPs in the myocardium are less understood. NPs exert their biological effects by binding to three distinct receptors, denoted NPR-A, NPR-B and NPR-C (Potter *et al*., 2006). NPR-A and NPR-B increase intracellular cGMP (a cyclic nucleotide important in cardiac ion channel regulation) levels by activating guanylyl cyclase (GC) enzymes (Potter & Hunter, 2001). cGMP can activate and/or inhibit important downstream signalling enzymes, including phoshodiesterases (PDE) and protein kinase G (PKG) (Potter *et al*., 2006). PDEs are critically involved in the regulation of cyclic nucleotide levels in the heart (Bender & Beavo, 2006). NPR-C, which binds all natriuretic peptides, is coupled to inhibitory G proteins (G_i) (Rose & Giles, 2008) that inhibit adenylyl cyclase (AC) enzymes and reduce intracellular cAMP (a cyclic nucleotide important in cardiac ion channel function) (Pagano & Anand-Srivastava, 2001).

Recently, a frameshift mutation in the *nppa* gene (which encodes ANP) was identified. The mutation results in the production of a 40 amino acid peptide, denoted

mutant ANP (mANP), whereas wild type (WT) ANP is a 28 amino acid peptide. Carriers of this mutation are characterized by the occurrence of atrial fibrillation in association with action potential (AP) shortening (Hodgson-Zingman *et al*., 2008). The receptor(s) and molecular mechanism responsible for the effects of mANP on atrial AP morphology are not known.

The goal of this study was to measure the effects of ANP and mANP on atrial myocyte electrophysiology and to determine the molecular mechanism responsible for these effects. The results of this study could significantly improve our understanding of the ionic and molecular mechanisms by which WT and mutant NPs regulate atrial myocyte electrophysiology. Furthermore, the experiments may provide novel insight into how NPs and their associated receptors affect AF susceptibility and may lead to new strategies for treating this common arrhythmia.

1.2 The Cardiac Action Potential

As major determinants of cardiac function, heart rate and contractility are important areas of study. Sinoatrial node (SAN) firing directly determines heart rate and contractility is dependent on intracellular calcium signalling, among other mechanisms. Thus, the study of cardiac electrophysiology of single isolated myocytes has proven to be an important technique in determining whole heart function and changes therein.

In the healthy human heart, the heart rate is determined by the intrinsic pacemaker, the SAN, where inward currents lead to a gradual diastolic depolarization that triggers an AP in the cell when a threshold potential is reached. The AP is then propagated throughout the atria and the atrioventricular node (AVN) to the ventricles leading to a coordinated

contraction of the myocardium. In 'working' myocytes of the atria (and ventricles) the AP is the result of inward sodium and calcium currents and outward potassium currents. The inward sodium current (I_{Na}) is responsible for the initial upstroke of the AP and is initiated by the depolarization of the cell membrane (Phase 0). The transient outward potassium current (I_{to}) produces a notch in the AP (Phase 1) which is followed by a plateau phase - the result of a balance between inward calcium current (I_{Ca}) and outward delayed rectifier potassium current (I_{Kur}) (Phase 2). As the calcium channels inactivate, the predominant outward potassium currents (I_{Kr}, I_{Ks} and I_{K1}) repolarize the cell (Phase 3) and I_{K1} is responsible for maintaining the resting membrane potential (Phase 4).

The data collected in this study are from mouse right atrial myocytes so it is important to note that Phase 1 and Phase 2 are difficult to distinguish in the mouse AP due to its speed (Nerbonne & Kass, 2005). Also the repolarizing currents I_{Ks} and I_{Kr} present in the human are not found in the mouse (Nerbonne, 2004).

Alterations in any of these currents can have profound effects on the AP and myocyte contractility, leading to cardiac dysfunction and arrhythmia. As we look for therapies to treat cardiovascular disease it is important to understand their implications in cardiac electrophysiology to ensure their success and safety.

1.3 The Cardiac L-Type Calcium Current

The cardiac voltage-gated L-type calcium channel (LTCC) provides the transient inward calcium current ($I_{Ca,L}$) responsible for maintaining depolarization of the myocyte during the phase 2 plateau of the AP (Schlotten *et al*., 2003). Atrial myocytes express both $Ca_v1.2$ and $Ca_v1.3$ α subunits which both contribute to total $I_{Ca,L}$ in the atria

(Koschak *et al*., 2001; Hatano *et al*., 2006; Qu *et al*., 2005; Zhang *et al*., 2005) (the structure and function of the LTCC subunits will be discussed further below in chapter 1.3.1). While $Ca_V1.2$ dependent $I_{Ca,L}$ activates at membrane potentials positive to -40 mV, $Ca_V1.3$ dependent $I_{Ca,L}$ activates at more negative membrane potentials (between -60 and -50 mV). Inactivation of $I_{Ca,L}$ is voltage and calcium dependent (Katz, 2011). LTCCs are also integral in converting the electrical signal into calcium influx to trigger downstream contraction events in a sequence termed excitation-contraction coupling.

1.3.1. Cardiac L-Type Channel Structure & Function

The LTCC is a multi-subunit protein made up of the pore-forming α_1 subunit and auxiliary subunits (β, $\alpha_2\delta$ and γ). The predominant $Ca_v1.2$ (α_{1C}) subunit has four homologous domains each containing six membrane-spanning segments connected through intracellular loops. Segments 1-4 contain the voltage sensor, while segments 5 and 6 form the pore and establish the ion specificity of the channel (Catterall, 2000). The C-terminus of the α_{1C} subunit is the site of modulation by signalling proteins (Dai *et al*., 2009) and is involved in channel trafficking to the cell surface (Fang & Colecraft, 2011). LTCCs containing the $Ca_v1.3$ (α_{1D}) subunit have also been found in the heart and contribute to SAN (Mangoni *et al*., 2003), AVN (Zhang & Kass, 2011) and atrial, but not ventricular, $I_{Ca,L}$ (Zhang *et al*., 2005). $Ca_v1.3$ contribution is unique because, compared to $Ca_v1.2$, it activates more rapidly and has a hyperpolarized activation potential (Koschak *et al*., 2001; Xu & Lipscombe *et al*., 2001).

The β subunit exists in four different isoforms (Buraei & Yang, 2010; Dolphin, 2003) of which only β_2 is present in the mouse heart (Meissner *et al*., 2011), while the canine

heart expresses all four (Foell *et al*., 2004). The human heart expresses three β isoforms; designated β_a, β_b and β_c (Collin *et al*., 1993). All isoforms contain a *src* homology domain and a guanylate-kinase domain separated by a HOOK domain (Chen *et al*, 2004; Opatowsky *et al*., 2004; Van Petegem *et al*., 2004). The guanylate-kinase domain contains the α_1 binding pocket that binds to a conserved sequence on the intracellular loop connecting domains I and II of the α_1 subunit (Pragnell *et al*., 1994). The β subunit modulates $I_{Ca,L}$ by increasing channel trafficking to the membrane (Fang & Colecraft, 2011) and preventing targeting to the proteasome (Altier *et al*., 2011; Waithe *et al*., 2011). The β subunit also modulates channel gating properties by increasing open channel probability, causing a hyperpolarizing shift in the voltage-dependence of activation and altering inactivation properties (Buraei & Yang, 2010; Dolphin, 2003).

The $\alpha_2\delta$ subunit, like the β subunit, is present in multiple isoforms (Bauer *et al*., 2010; Dolphin, 2012). Isoform 1 and 2 mRNA has been detected in the human heart and isoform 3 has been found in rat atria (Fuller-Bicer *et al*., 2009). The α and δ subunits are held together by a disulfide bond (Bauer *et al*., 2010; Dolphin, 2012). The α_2 subunit is entirely extracellular, while the δ subunit has a short hydrophobic region that transverses the membrane tethering the whole $\alpha_2\delta$ subunit to the membrane (Bauer *et al*., 2010). Similar to the β subunit, the $\alpha_2\delta$ subunit increases $I_{Ca,L}$ amplitude and modulates current kinetics and voltage-dependence (Bangalore *et al*., 1996; Gao *et al*., 2000).

The γ subunit has 8 isoforms (Chu *et al*., 2001) but only one (isoform 6) has been confirmed to be present in the rat heart. Heterologous expression studies using γ isoforms 4, 6, 7 and 8 have shown effects on current amplitude and gating properties unique to

each isoform and which appear to also depend on the isoform of the β subunit (Yang *et al*., 2011). The functional impact of the γ subunit in the heart is not well known.

The LTCC is also associated with the calcium sensing protein calmodulin (Peterson *et al*., 1999; Zuhlke *et al*., 1999). This association allows the channel to undergo negative and positive feedback based on intracellular calcium ion levels (Halling *et al*., 2005). At resting intracellular calcium levels, calmodulin is associated with the $Ca_v1.2$ channel (Erickson *et al*., 2001), where in addition to its calcium-dependent regulation, it also targets the channel to the cell surface (Wang *et al*., 2007).

1.3.2 Cardiac L-Type Calcium Current Dysregulation & Disease

Mutations in LTCC proteins are associated with a variety of diseases that can manifest as cardiac arrhythmias and/or cause heart failure (Shaw & Colecraft, 2013). Gain-of-function mutations lead to a loss of channel inactivation and result in calcium overload. For example, Timothy syndrome is linked to a gain-of-function mutation which is characterized by a long QT interval, ventricular arrhythmias and structural alterations in the heart (Splawski *et* al., 2004; Splawski *et al*., 2005). In comparison, loss-of-function mutations in $Ca_v1.2$ have been linked to Brugada syndrome characterized by a short QT interval and sudden death. Mutations implicated in the loss-of-function phenotype are linked to inhibition of the β subunit, reduced $I_{Ca,L}$ and decreased channel conductance and alterations in inactivation kinetics (Antzelevitch *et al*., 2007). Zhang *et al*. demonstrated that $Ca_v1.3$ calcium channel deficient mice ($Cav1.3^{-/-}$) also display cardiac dysfunction. As discussed in chapter 1.3.1, $Ca_v1.3$ contributes to a hyperpolarized shift in activation of the LTCC, so $Ca_v1.3^{-/-}$ mice are characterized by depolarized activation potentials. The

$Ca_v1.3^{-/-}$ mice also demonstrated atrial arrhythmia such as inducible atrial fibrillation (Zhang *et al*., 2005). Reduced $I_{Ca,L}$, a major mechanism for AF susceptibility and maintenance, has been implicated in chronic human atrial fibrillation (Van Wagoner *et* al., 1999) and documented in rapidly paced canine atria (Yue *et al*., 1999) (this will be discussed further in the chapter 5: discussion).

1.4 Natriuretic Peptides

Natriuretic peptides (NPs) are an essential family of hormones found in many species with effects throughout the body (Kuhn, 2004; Levin *et al*., 1998). Their investigation began in the 1980's with the observation of rapid diuresis and natriuresis following the injection of atrial tissue homogenates into the rat (de Bold *et al*., 1981). Subsequent studies identified the 'factor' responsible for this response and determined that it was a peptide hormone stored in atrial granules. The peptide was initially named atrial natriuretic factor and subsequently renamed ANP.

The NP family consists of four structurally homologous, but genetically distinct, members; atrial natriuretic peptide (ANP) (de Bold *et al*., 1981), B-type natriuretic peptide (BNP) (Sudoh *et al.*, 1988), C-type natriuretic peptide (CNP) (Sudoh *et* al., 1990) and *Dendroaspis* natriuretic peptide (DNP) (Schweitz *et al.*, 1992) (Fig. 1.1). All members of the NP family contain the sequence CFGXXXDRIXXXXGLGC (where X symbolizes any amino acid). The terminal cysteines (represented by the 'C') covalently bond forming a disulfide-linked ring structure. While this ring structure is highly conserved, the two terminal amino acid chains (i.e. NH_2- and -COOH) are highly variable among the members, with differences in both length and amino acid sequence (Misono *et*

Figure 1.1: Schematic representation of natriuretic peptide amino acid sequence and ring structure. ANP: atrial natriuretic peptide; BNP: B-type natriuretic peptide; CNP: C-type natriuretic peptide; DNP: *Dendroaspis* natriuretic peptide.

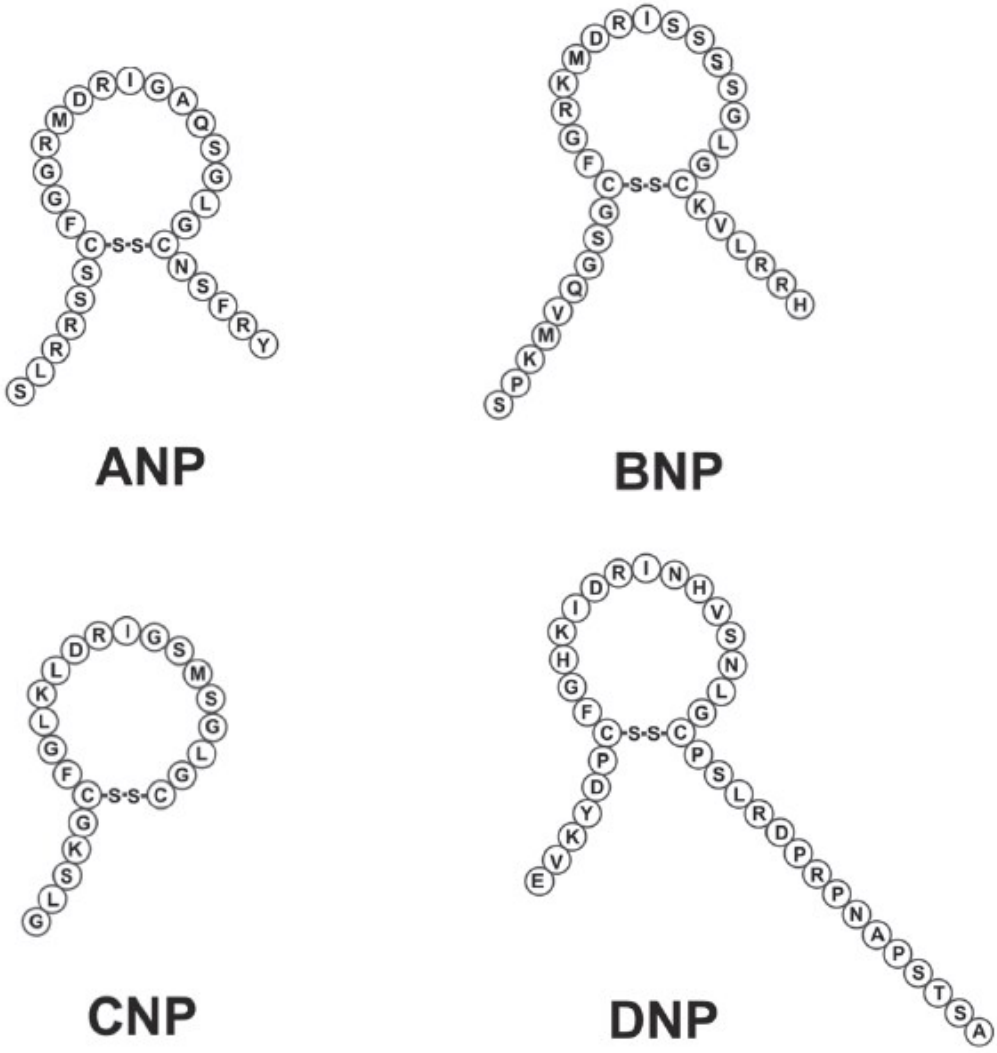

Figure 1.1

al., 1984). In terms of WT NPs, this study focuses on ANP and therefore only its details will be discussed further.

1.4.1 ANP Synthesis & Processing

The genetic segregation of the NPs results in tissue distribution and regulation properties exclusive to each peptide. The human ANP gene (*nppa*) is located on chromosome 1p36.2 and contains three exons (Yang-Feng *et al*., 1985). Pre-pro-ANP is 151 amino acids in length. Cleavage at the amino terminal end results in the 126 amino acid pro-ANP. Pro-ANP is produced and stored primarily in the atria of the heart in distinct granules within cardiomyocytes (Potter *et al*., 2006). Stretch in the atrial wall as a result of increased intravascular volume is the primary cause of pro-ANP release (Edwards *et al*., 1988). Upon secretion pro-ANP is quickly cleaved by a protease, corin, to produce the mature 28 amino acid ANP (Potter *et* al., 2006; Yan *et al*., 2000). ANP release into the coronary sinus allows it to circulate throughout the body to reach its target organs. *Nppa* is also expressed in the kidney where different processing results in production of a protein called urodilatin which plays a local regulatory role on kidney function (Schulz-Knappe *et al*., 1988). Plasma ANP levels in healthy patients are approximately 10 fmol/ml (Cody *et al*., 1986).

1.4.2 ANP Metabolism, Clearance & Degradation

Natriuretic peptides have relatively short half-lives (i.e. the half- life for human ANP is 2.5 minutes) resulting in rapid clearance following their synthesis and release (Yandle *et al*., 1986). NPs can be excreted through the renal system, however this process has

been shown to play an insignificant role in the regulation of NP circulating levels (Shima *et al*., 1988). There are two other processes in which NPs are expected to leave the circulation and lose their biological function.

The first process is clearance through receptor-mediated internalization. This mechanism is primarily associated with NPR-C. However, all NPRs are able to remove NPs from circulation by binding (Maack *et* al., 1987). Upon ligand binding, NPR-C is thought to internalize NPs through a clathrin-dependent lysosomal hydrolysis mechanism (Nussenzveig *et al*., 1990). This has resulted in NPR-C being originally classified as a 'clearance receptor' with no signalling functions. NPR-C is now known to activate signalling pathways (see chapter 1.5.2 below for further details). Evidence suggests that NPR-A and NPR-B are not triggered by NP binding to internalize or degrade but this remains controversial (Fan *et al*., 2004).

The second process by which ANP is removed from the circulation is degradation by extracellular proteases. These proteases show NP and species specificity. Neprilysin, enkephalinase and CD10 have all been implicated in NP degradation but enkephalinase (also known as neutral endopeptidase 24.11) seems to play the largest role (Erdos & Skidgel, 1989; Kenny *et al*., 1993; Soleilhac *et al*., 1992). Insulin degrading enzymes have also shown involvement in the degradation of ANP (Potter *et al*., 2011).

Figure 1.2: Schematic representation of the natriuretic peptide receptors and their respective ligands. NPR-A, NPR-B, NPR-C: natriuretic peptide receptor type A, B, C, ANP; atrial natriuretic peptide, BNP; B-type natriuretic peptide; CNP; C-type natriuretic peptide; DNP; *Dendroaspis* natriuretic peptide; cANF; selective natriuretic peptide receptor C agonist, cGMP; cyclic guanosine monophosphate, G_i; inhibitory G-protein.

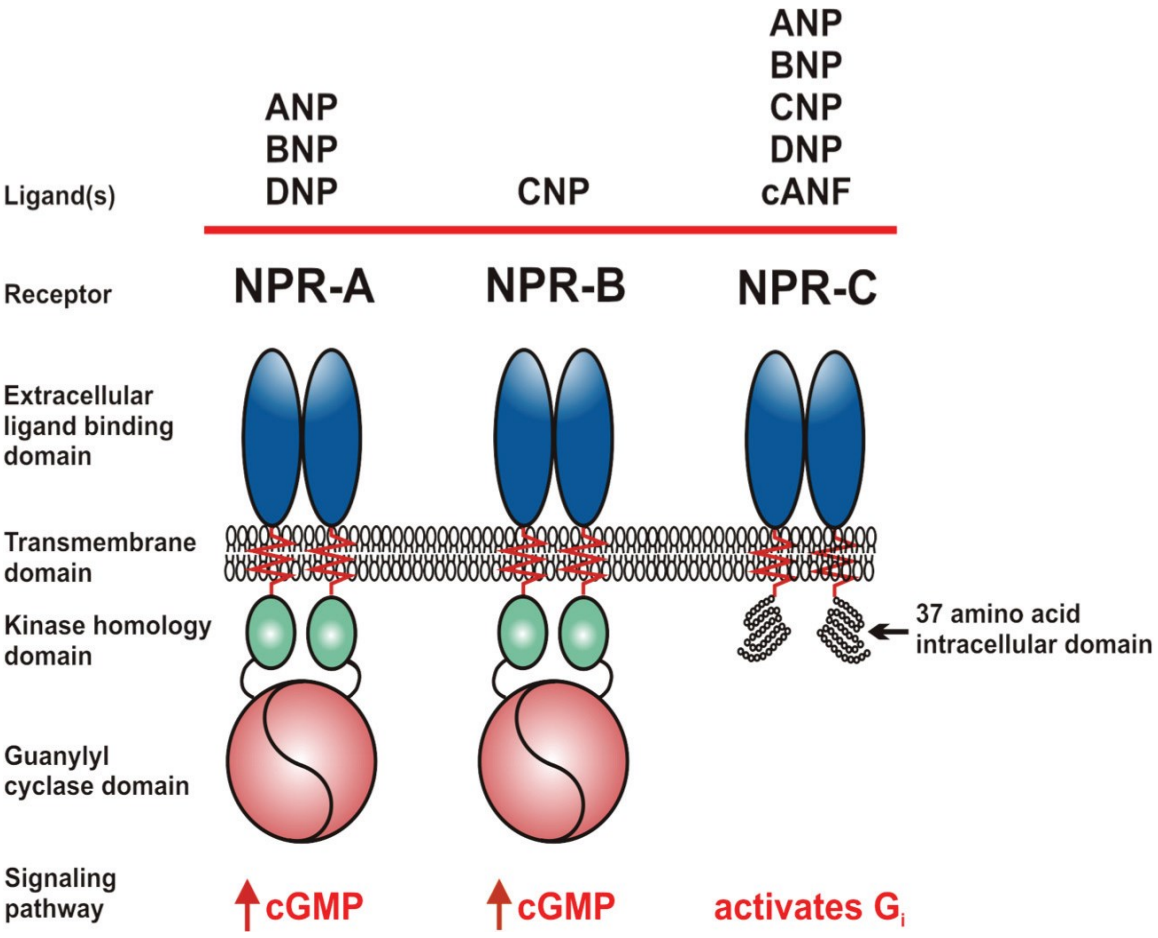
Ligand(s)
ANP
BNP
DNP
CNP
ANP
BNP
CNP
DNP
cANF
Receptor
NPR-A
NPR-B
NPR-C
Extracellular ligand binding domain
Transmembrane domain
Kinase homology domain
Guanylyl cyclase domain
37 amino acid intracellular domain
Signaling pathway
cGMP
cGMP
activates G_i

Figure 1.2

1.5 Natriuretic Peptide Receptors

There are three known natriuretic peptide receptors (NPRs) through which NPs elicit their effects (Fig. 1.2). ANP is only known to bind to NPR-A and NPR-C physiologically so only these receptors will be discussed further.

1.5.1 Natriuretic Peptide Receptor A

Natriuretic peptide receptor A (NPR-A) is expressed in multiple tissue types, including adrenal, brain, vascular smooth muscle, lung, kidney, adipose and heart (Lowe *et al*., 1989; Nagase *et* al., 1997; Schultz *et al*., 1989). NPR-A is the primary receptor for ANP, BNP (Lucas *et al.,* 2000) and DNP (Johns *et al*., 2007). The 16 kilobase human NPR-A gene is located on chromosome 1q21-22 and includes 22 exons and 21 introns (Lowe *et al*., 1989; Takahashi *et al.,* 1998). NPR-A is a guanylyl cyclase (GC) linked receptor consisting of an approximately 450 amino acid extracellular ligand binding domain at the amino terminus, a 20 to 25 amino acid transmembrane domain and an intracellular domain. The intracellular domain contains a 250 amino acid kinase homology domain (KHD), a 40 amino acid dimerization domain and a 450 amino acid GC domain at the carboxyl terminus (Potthast & Potter, 2005). In terms of NPR-A activation, ANP, BNP and DNP (Johns *et al*., 2007) have similar binding affinities, while the binding affinity of CNP is much less (Suga *et al*., 1992).

NPR-A is phosphorylated in its basal state allowing for activation. Upon ligand binding, NPR-A undergoes an adenosine triphosphate (ATP) dependent conformational change which removes the KHD's inhibitory role over the GC (Jewett *et al*., 1993). The GC is now free to catalyze the conversion of guanosine triphosphate (GTP) to cyclic

guanosine monophosphate (cGMP) (Potter & Hunter, 2001). The binding of ANP to NPR-A increases cGMP in a time- and concentration-dependent manner (Chinkers *et al*., 1989; Schultz *et al.,* 1989).

Dephoshorylation of NPR-A leads to its desensitization in response to prolonged NP exposure or protein kinase C (PKC) activation. The occurrence of NPR-A internalization and degradation through a lysosomal pathway remains controversial (Foster & Garbers, 1998; Potter & Garbers, 1992; Potter & Garbers, 1994).

1.5.2 Natriuretic Peptide Receptor C

Natriuretic peptide receptor C (NPR-C) is found in most tissues, including brain, adrenal, kidney, heart and vascular smooth muscle (Anand-Srivastava *et al*., 1985; Anand-Srivastava *et al*., 1986; Anand-Srivastava *et al*., 1991; Anand-Srivastava, 2005; Bianchi *et al*., 1986; Féthière *et al*., 1992; de Léan *et al*., 1984). NPR-C is known to bind all four NPs (Bennett *et al*., 1991). The human NPR-C gene is located on chromosome 5p13-14 and contains 8 exons and 7 introns. The gene is relatively large spanning 65 kilobases (Rahmutula *et al*., 2002). NPR-C shares the extracellular ligand binding domain and transmembrane domain structures with NPR-A. Intracellularly, however, NPR-C lacks the KHD and GC-linked domain (Porter *et al*., 1990). Instead it contains a 37 amino acid intracellular domain containing inhibitory G protein (G_i) activator sequences (Pagano & Anand-Srivastava, 2001). Upon ligand binding, G_i directly inhibits adenylyl cyclase (AC) activity (Anand-Srivastava & Trachte, 1993; Rose *et al*., 2003; Rose *et al*., 2004) in a GTP dependent manner (Anand-Srivastava *et al*., 1996). NPR-C has also been shown to interact with phospholipase C β (PLCβ) (Pagano & Anand-Srivastava, 2001). This interaction increases diacylglycerol (DAG) and inositol triphosphate (IP_3)

production leading to an increase in intracellular Ca^{2+} concentrations (Anand-Srivastava *et al*., 2005). In terms of binding affinity for NPR-C, ANP and DNP (Kim *et al*., 2011) have greater than or equal affinity as CNP and BNP has less affinity than CNP (Suga *et al*., 1992).

NPR-C's historical role as "the clearance receptor" designates its primary function as internalization and degradation following ligand binding in order to clear NP from the circulation (Jaubert *et* al., 1999; Matsukawa *et al*., 1999). While this process may still serve a regulatory purpose, the role of NPR-C in signalling through G_i and PLCβ is clear.

1.6 Natriuretic Peptide Signalling

The binding and activation of the NPRs by their respective NPs leads to a complex downstream signalling pathway involving many important proteins and an intricate cross talk between generated cyclic nucleotides (Fischmeister *et al*., 2006). The variety of physiological effects that result are dependent on the pattern of expression of the NPRs and downstream signalling molecules throughout the body. Activation of NPR-A initiates the activity of its associated GC, thus increasing intracellular cGMP levels. cGMP interacts with the cGMP- dependent protein kinase G (PKG), phoshodiesterases (PDEs) and cyclic nucleotide-gated ion channels (Baxter, 2004; Potter *et al*., 2006). PKG is a serine-threonine kinase that exists in two isoforms (Baxter, 2004) denoted PKGI and PKGII. PKGI is found in the cytosol of platelets, smooth muscle cells, cardiomyocytes and brain cells. In contrast, PKGII is found membrane-bound in the intestine, kidney, brain, chrondrocyte and bone (Smolenski *et* al., 1998). PKGI is known to effect important cardiac ionic currents such as increasing the calcium-sensitive potassium currents (Alioua

et al., 1998; Swayze & Braun, 2001) and decreasing L-type calcium currents (Kojda *et al.* 1996; Levi *et al.* 1989; Méry *et al.* 1991; Sumii & Sperelakis, 1995; Wahler & Dollinger, 1995).

PDEs, which are the enzymes responsible for degradation of cyclic nucleotides (cAMP and cGMP), play an essential role in the NPR-A signalling pathway (Potter *et al*., 2006). There are 11 PDE families grouped based on their sequence, substrate specificity and regulatory properties (Bender & Beavo, 2006; Beavo, 1995; Conti & Beavo, 2007; Francis *et al.*, 2001; Francis *et al.*,2011; Maurice *et al.*, 2003) and 7 of these PDE families have been described in the heart: PDE1, PDE2, PDE3, PDE4, PDE5, PDE8 and PDE9 (Kostic *et al.*, 1997; Loughney *et al.*, 1996; Meacci *et al.*,1992; Onody *et al.*, 2003; Senzaki *et al.*, 2001; Soderling & Beavo, 2000; Soderling *et al.*,1998). PDE1-3 are able to degrade both cAMP and cGMP. PDE4 and PDE8 are capable of degrading only cAMP, while PDE5 and PDE9 degrade only cGMP (Lugnier, 2006; Zaccolo & Movesian, 2007). In addition to cGMP's role as a PDE substrate, PDEs can also be regulated by cGMP. For example, PDE5 can be bound allosterically by cGMP which will increase its activity and increase cGMP degradation in a feed-forward mechanism. This allosteric regulation also facilitates crosstalk between cGMP and cAMP. For example, PDE2 is activated by cGMP and functions to enhance cAMP degradation, while PDE3 is inhibited by cGMP, which results in less degradation of cAMP (Omori & Kotera, 2007; Zaccolo & Movesian, 2007). PDEs have been found to exist in subcellular microdomains based on their own individual spatial and temporal localization within the cell (Fischmiester *et* al., 2006; Maurice *et al*., 2003; Movesian, 2002; Hua *et al*., 2012; Zaccolo, 2011; Zaccolo & Movesian, 2007). This adds even further complexity to their

regulatory role as different concentrations of cyclic nucleotides effect different PDEs. For example, cGMP at a lower concentration inhibits PDE3, while at higher concentrations cGMP activates PDE2, leading to an increase or decrease in cAMP levels, respectively (Vandecasteele *et al*., 2001). In the context of NP signalling, cGMP-cAMP crosstalk allows communication between all three NPRs. While NPR-A and NPR-B are linked to GC activity to control cGMP levels, NPR-C's signalling through G_i effects AC activity and, subsequently cAMP concentration (Anand-Srivastava *et* al., 1993; Rose *et al*., 2003; Rose *et al*., 2004). The principal downstream target of cAMP is protein kinase A (PKA) (Zaccolo & Movesian, 2007). PKA has also been shown to have role in regulating the activity of PDE1, PDE3, PDE4 and PDE5 (Omari & Kotera, 2007).

Both cAMP and cGMP are able to bind to cyclic nucleotide-gated ion channels to mediate additional cellular responses (Potter *et al*., 2006). These channels are non-selectively permeable to cations (Kaupp & Seifert, 2002) and are most prominent in sensory cells, the brain, airway epithelial cells and kidney. There has been no evidence of a direct link between these channels and NPs; however, they are worth noting due to the wide distribution of NPRs and their effects on circulating cyclic nucleotide levels (Potter *et al*, 2006).

1.7 Physiological Effects of Natriuretic Peptides

NPs have a variety of effects throughout the body that can be classified as both paracrine and endocrine. NPs are most commonly associated with their diuretic and natriuretic effects (D'Souza *et al*., 2004; Kuhn, 2004; Levin *et al*., 1998), but they can also regulate cardiac hypertrophy and fibrosis, vascular relaxation and remodelling,

pulmonary hypertension, the renin-aldosterone system, fat metabolism, long bone growth and processes in the brain and immune system (Potter *et al*., 2006). Their effects are particularly evident when disease occurs subsequent to genetic alteration (Kuhn, 2004). Given the focus of this thesis on ANP, only NP effects mediated through NPR-A and NPR-C in the cardiovascular system will be discussed.

1.7.1 Effects on Blood Pressure

ANP plays a predominant role in blood pressure homeostasis shown clearly through the inverse linear relationship between NPR-A gene copy number and blood pressure in mice (Oliver *et* al., 1998). The effects of ANP and NPR-A on blood pressure were defined using transgenic mice either lacking ANP or NPR-A or mice expressing higher than normal levels of ANP. In the first case, blood pressure measured in transgenic mice lacking functional ANP was 20 to 40 mmHg higher than control (John et al. 1995; John et al. 1996). Lack of functional NPR-A in mice also results in hypertension (Lopez *et* al., 1995; Lopez *et* al., 1997; Oliver *et* al., 1997). In contrast, mice expressing larger than normal levels of ANP had a blood pressure 20 to 30 mm Hg lower than control (Ogawa et al. 1994; Steinhelper et al. 1990). Over-expression of NPR-A also results in hypotension (Oliver *et al*., 1998). Over-expression of BNP, which also activates NPR-A, produces arterial hypotension similar to ANP (Ogawa *et* al., 1994). Interestingly, mice lacking functional NPR-C receptors were reported to have modestly lower systolic and diastolic blood pressure (Matsukawa *et al*., 1999).

Blood pressure regulation by ANP is due to the combined effects on intravascular volume, vasorelaxation, natruiresis and diuresis. Through NPR-A, ANP is able to

increase diuresis and natriuresis by inhibiting the renin-angiotensin-aldosterone system (RAAS) (Richards *et al*., 1988). The RAAS is a hormone system that regulates blood pressure and fluid homeostasis. The liver secretes angiotensinogen which is converted by the enzyme renin to angiotensin I. Angiotensin I is then converted to angiotensin II (Ang II) by angiotensin converting enzyme (ACE). Ang II acts on the adrenal cortex to trigger release of aldosterone. Ang II also causes vasoconstriction. Aldosterone acts on the collecting ducts of the kidney to decrease sodium and water excretion effectively increasing fluid volume. ANP decreases renin secretion and subsequently aldosterone release, thus increasing natriuresis and diuresis (Hunt *et al*., 1996; Potter *et al*., 2006; Wijeyaratne & Moult, 1993). NPR-A activation also increases glomerular filtration rate by constricting the efferent arteriole and dilating the afferent arteriole causing a rise in glomerular capillary pressure (Marin-Grez *et al*., 1986). The hypotensive response can also be partly attributed to the reduction in intravascular volume due to an ANP/NPR-A mediated increase in capillary permeability (Huxley *et al*., 1987; McKay & Huxley, 1995). In addition ANP is able to promote vascular relaxation in a PKGI-dependent manner as a result of its effects on downstream calcium signalling (Carvajal *et al*., 2000; Hofmann *et al*., 2000).

1.7.2 Effects on the Heart

Transgenic mice have provided powerful insight into the effects of NPs on the heart. Mice without functioning ANP (John *et al*., 1995) or NPR-A (Franco *et al*., 1998; Kishimoto *et* al., 2001; Oliver *et al*., 1997) have an enlarged heart. This hypertrophic response is due to both hypertension effects and the loss of an inhibitory effect on local

growth (Knowles *et al*., 2001). In contrast, over-expression of ANP results in a smaller heart (Barbee *et* al., 1994; Steinhelper *et al*., 1990). Both ANP and BNP signalling through NPR-A are able to reduce pressure-induced cardiac remodelling (Tamura *et al*., 2000; Knowles *et al*., 2001; Holtwick *et al*., 2003; Tsuneyoshi *et al*., 2004). The BNP/NPR-A pathway is predominantly involved in decreased fibrosis (Cao & Gardner, 1995). The mechanism is still controversial but seems to entail alterations in mitogen-activated protein kinase (Kapoun *et al*., 2004; Takahashi *et al*., 2003) and matrix metalloproteinase activity **(**Kapoun *et al*., 2004; Tsurda *et al*., 2002; Wang *et al*., 2003). BNP gene deletion results in cardiac fibrosis (Tamura *et al*., 2000). Lack of functional NPR-A in mice has also been shown to result in cardiac hypertrophy as well as sudden cardiac death (Lopez *et* al., 1995; Lopez *et* al., 1997; Oliver *et* al., 1997).

Experiments on single isolated cardiomyocytes have identified additional roles for NPs in cardiac physiology. In most cases the effect of NPs are concentration and/or species-dependent, and can be influenced by experimental protocol. Application of ANP, BNP and CNP to isolated rabbit ventricular myocytes revealed a concentration-dependent decrease in myocyte contractility that was dependent on cGMP (Zhang *et al*., 2005). This result was reproduced in an isolated perfused mouse working heart model with CNP, but not ANP (Pierkes *et al*., 2002).

More recently, work from our laboratory has shown NP effects on SAN and atrial electrophysiology in isolated hearts and myocytes isolated from mice. BNP elicited a dose-dependent increase in heart rate and conduction throughout the atria. In support of this observation, BNP (100 nM) increased spontaneous AP frequency in isolated SAN myocytes. The change in frequency was due to an increase in $I_{Ca,L}$ and the

hyperpolarization-activated current (I_f). BNP was also shown to increase $I_{Ca,L}$ and AP duration (APD) in atrial myocytes in the presence of the β-adrenergic receptor (β-AR) agonist isoproterenol (ISO; 10nM), but not in basal conditions. Using atrial myocytes isolated from mice lacking functional NPR-C (NPR-$C^{-/-}$), the effects of BNP were maintained. In contrast, in the presence of the NPR-A blocker A71915, the effects of BNP on SAN myocytes was lost. The BNP effects (in the presence of ISO) in atrial myocytes were also lost with the addition of A71915. This reveals that the effects of BNP were through NPR-A activation. Interestingly, in the presence of the PDE3 inhibitor, milrinone, the effects of BNP were absent indicating that their effects occur in a PDE3-dependent fashion (Azer *et al*., 2012; Springer *et al.,* 2012).

In the presence of a maximal dose of ISO (1 μM), BNP switches to decreasing heart rate (in Langendorff-perfused mouse hearts) and decreasing AP firing in SAN myocytes. The NP induced decrease in heart rate and SAN firing was absent in NPR-$C^{-/-}$ hearts (Azer *et* al., 2012). This NPR-C inhibitory effect of NPs is due to a decrease in $I_{Ca,L}$ in isolated SAN myocytes (Rose *et al*., 2004). This effect is mirrored in frog atrial myocytes, where in the presence of ISO (100nM), APD is shortened due to an inhibition of $I_{Ca,L}$ through NPR-C activation (Rose *et al*., 2003).

The effects of BNP on $I_{Ca,L}$ through NPR-A and NPR-C have been very well studied, however the effect of ANP through these receptors is less known. While it is known that $I_{Ca,L}$ is regulated by ANP (Tohse *et al*., 1995), whether it modulates inotropy or chronotropy, and how, is controversial. Negative chronotropic effects of ANP on the heart have been proposed by multiple groups. The mechanism for these effects has been linked to intracellular cGMP production and the activation of PKGI leading to a decrease

in $I_{Ca,L}$ (Doyle *et al*., 1997; McCall & Fried, 1990; Tajima *et al*., 1998; Tohse *et al*., 1995). In early developmental cardiomyocytes a decrease in $I_{Ca,L}$ following ANP application was mediated by cGMP and the activation of PDE2, which resulted in a decrease in PKA activity (Miao *et al*., 2010). An ANP induced a decrease in $I_{Ca\,L}$ has also been reported in guinea pig ventricle (Levi *et al*., 1989), chick embryo (Bkailey *et al*., 1993), human atrial (Le Grand *et al*., 1992) and rabbit ventricular cardiomyocytes (Tohse *et al*.,1995). In contrast, other studies have reported that ANP can elicit a positive chronotropic response (Lainchbury *et al*., 2000). Interestingly, in frog cardiomyocytes ANP had no effect on basal $I_{Ca,L}$, but after pre-stimulation with a β-AR agonist ANP decreased $I_{Ca,L}$ (Gisbert & Fischmeiter, 1988).

It is likely that differing patterns of results, as described above, are due to the complexity of NP signalling in the heart, which can involve multiple receptor subtypes and downstream signalling molecules, which may make unique contributions in different physiological conditions.

1.8 Atrial Natriuretic Peptide & Atrial Fibrillation

Atrial fibrillation (AF) is the most common irregular heart rhythm (arrhythmia) treated in emergency rooms (Fuster, *et al*., 2011) and is estimated to affect 1-2% of the population (Stewart, *et al*., 2001) – which is approximately 350, 000 Canadians. AF is characterized by a fast and irregular beating of the heart's atria. Due to the dyssynchrony of the beats, or atrial contractions, pooling of blood in the atria is common and often leads to the formation of clots. As a result, AF is associated with a 3 to 5 fold greater risk of ischemic stroke (Heart & Stroke Foundation, 2013). The incidence of AF doubles with

every decade over age 55 (Benjamin, *et al*., 1994) and with Canada's aging population it is clear that unraveling the mechanisms of AF is very important for the prevention and proper treatment of this disease.

In 2008, Hodgson-Zingman *et al*. published a linkage analysis of a white family of northern European ancestry who had an autosomal dominant AF phenotype. Genetic mapping traced the AF locus to chromosome 1p36-p35 and a heterozygous frameshift mutation was discovered in the ANP gene, *nppa*. The 2 base pair deletion abolishes a normal stop codon and results in a 12-amino acid (sequence; RITAREDKQGWA) extension of the carboxyl terminus of ANP (Fig. 1.3). This mutant form of ANP (mANP) was found in the circulating plasma of all affected family members at 5- to 10- fold higher concentrations than WT ANP, but not found in unaffected family members or unrelated control subjects (Hodgson-Zingman *et al*., 2008). The increased mANP plasma levels were determined to be due to a resistance to proteolytic degradation compared to wildtype ANP. The half-life of mANP was 4.5 minutes, nearly twice as long as WT ANP. The primary enzyme responsible for mANP degradation appears to be a serine protease, while ANP is predominantly degraded by a neutral endopeptidase as described above in chapter 1.2.2. Interestingly, while the neutral endopeptidase was able to fully inactivate WT ANP, mANP activity was only 35% reduced after a 30 minute application of the enzyme. Therefore, the 12 amino acid extension appears to significantly affect the properties of mANP degradation (Dickey *et al*., 2009).

As a preliminary mechanistic investigation, Hodgson-Zingman *et al*., also studied the effects of mANP in a rat isolated whole-heart model. They noticed, in comparison to WT ANP, mANP significantly shortened the monophasic APD at 90% repolarization. This

Figure 1.3: Amino acid sequence and structure of atrial natriuretic peptide and mutant atrial natriuretic peptide. ANP: atrial natriuretic peptide; mANP: mutant atrial natriuretic peptide.

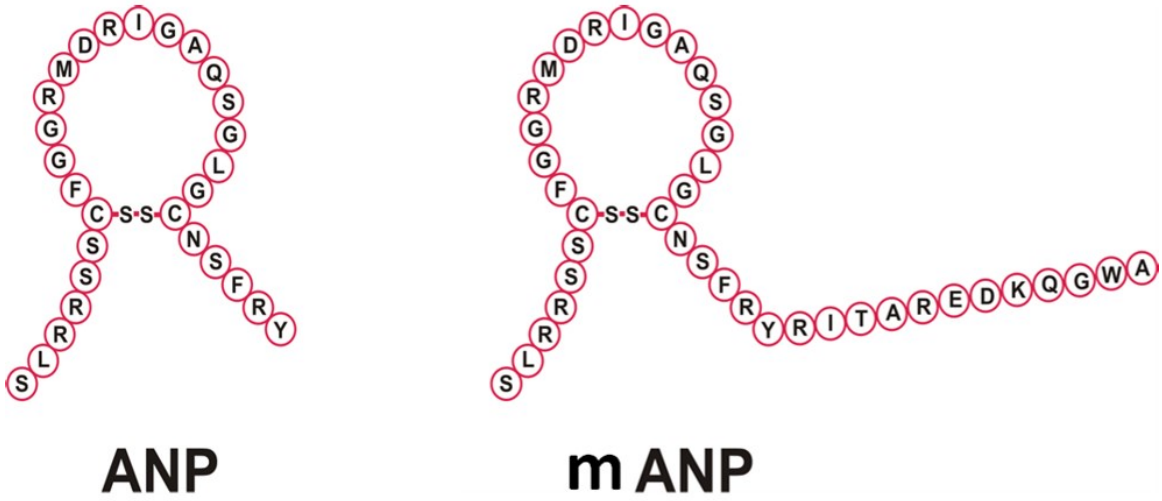

Figure 1.3

corresponded to a decrease in the effective refractory period (ERP) upon mANP application compared to WT ANP (Hodgson-Zingman *et al*., 2008). Dickey *et al*. further characterized mANP and showed a receptor binding profile similar to ANP; mANP bound human NPR-A and NPR-C with the same affinity as ANP (IC_{50}:1.6 nM with WT ANP; IC_{50}:2.4 nM with mANP). Whole cell activation of human NPR-A was also similar (EC_{50}:12.5 nM with WT ANP; EC_{50}:11.6 nM with mANP). Interestingly, at the highest concentration (10 μM), mANP stimulated significantly higher cGMP production by NPR-A than ANP (~1150 pmol cGMP with mANP versus ~800 pmol cGMP with ANP). However, at all other concentrations the potency of ANP and mANP was comparable. A reduced affinity and potency of mANP for rat NPR-A was observed. It was remarked that this reduction, though significant, was small. Another difference between ANP and mANP was that mANP had a slightly greater ability to activate NPR-B. The EC_{50} values for mANP and WT ANP were 800 nM and 1200 nM, respectively. The maximum activity with mANP was also 50% greater than with WT ANP. However, ANP and mANP had similarly low cGMP production by NPR-B relative to the primary ligand CNP (EC_{50} values were 32 nM, 28 nM and 142 nM for WT ANP, mANP and CNP, respectively). The ability to bind NPR-C was also the same for WT ANP and mANP (IC_{50} values for WT ANP and mANP were 2.4 nM and 3.2 nM, respectively) (Dickey *et al*., 2009).

Currently, mANP's physiological effects and role in AF appear to be due to its greater circulating concentration (Hodgson-Zingman *et al*., 2008). To my knowledge, there have been no experiments done to evaluate mANP effects on cardiac ion channels.

1.9 Purpose & Hypothesis

The effects of ANP on cardiac ion channels have been variable due to species and technique variations used in its investigation (Perrin & Gollob, 2012). ANP has the ability to bind both NPR-A and NPR-C, which can mediate opposing effects on cAMP production (Azer *et al*., 2012). NPR-A activation increases intracellular cGMP, which modulates several downstream signalling processes as described earlier (Potter *et al*., 2006). NPR-C is linked to G_i and the inhibition of AC activity, which reduces cAMP signalling (Anand-Srivastava *et al*., 1987; Rose *et al*., 2003; Rose *et al*., 2004; Rose *et al*., 2005). The conflicting effects of ANP on cardiac function and myocyte electrophysiology may be due to the complex involvement of PDEs and the subsequent cross talk between cAMP and cGMP pathways in different physiological conditions (Zaccolo & Movesian, 2007).

Similar to ANP, mANP has been shown to bind NPR-A and NPR-C and stimulate cGMP production through NPR-A (Dickey *et al*., 2009). One study also showed a decrease in monophasic APD upon mANP application (Hodgson-Zingman *et al*., 2008), however, no other electrophysiological mechanisms have been studied. Patients with the ANP mutation have also shown a predisposition to AF (Hodgson-Zingman *et al*., 2008). While knowledge has greatly increased, AF still contributes significantly to population morbidity and mortality and current therapies have major limitations (Dobrev & Nattel, 2010). The study of mANP could improve mechanistic understanding of AF and provide insight for future therapies.

Therefore, based on previous studies investigating the electrophysiological effects of NPs in the heart, this research set out to further investigate the electrophysiological

effects of ANP and mANP in mouse right atrial myocytes, and to clarify the involvement of NPRs in these effects.

It was hypothesized that ANP would have no effect on atrial APD or atrial $I_{Ca,L}$ in basal conditions. However, in the presence of ISO, ANP would be expected to increase atrial APD and atrial $I_{Ca,L}$ through NPR-A activation similar to the results obtained previously with BNP in mouse right atrial myocytes (Springer *et al*, 2012). Increased levels of cGMP (following NPR-A activation) can result in the inhibition of PDE3 activity which would reduce the hydrolysis of cAMP. Accordingly, it was further hypothesized that ANP would elicit an increase in intracellular cAMP in atrial myocytes the presence of ISO (Omori & Kotera *et al*., 2007; Zaccolo & Movesian *et al*., 2007).

No studies have investigated the ionic mechanisms by which mANP affects atrial electrophysiology. We hypothesized that mANP would have unique electrophysiological effects on atrial $I_{Ca,L}$, which could at least partially explain how this mutant peptide increases susceptibility to AF.

CHAPTER 2: MATERIALS AND METHODS

2.1 Experimental Animals

All experimental procedures were done in accordance with the regulations of The Canadian Council on Animal Care and were approved by Dalhousie University.

2.1.1 C57BL/6 Mice

The mice used in this study were male, between 10 and 14 weeks of age. C57BL/6 mice (Charles River) were used to study the effects of ANP and mANP in a WT phenotype.

2.1.2. NPR-C Mutant Mice

To study the role of NPR-C, mice lacking a functional NPR-C receptor (NPR-$C^{-/-}$) were used (strain: B6; C-*Npr3lgj*/J; Jackson Laboratories). This strain was backcrossed into a C57BL/6 background for more than 10 generations. The NPR-$C^{-/-}$ mice contain an in-frame 36 base pair deletion between positions 195 and 232 on chromosome 15. This mutation leads to a non-functional NPR-C protein that is lacking 12 amino acids in the extracellular domain (Jaubert *et al*., 1999). All NPR-$C^{-/-}$ mice were male and between the ages of 10-14 weeks.

2.2 Mouse Right Atrial Myocyte Isolation

Single cells were isolated from the right atrial appendage from the hearts of adult male C57BL/6 mice or NPR-$C^{-/-}$ mice using previously described techniques (Rose *et al.*, 2007). In summary, adult mice were injected intraperitoneally with 0.2 mL of heparin to

prevent clotting. The heparin was allowed to circulate for 5 minutes. The mice were then anesthetized with isoflurane and sacrificed. The right atrial appendage was removed from the heart and placed in a dissecting dish containing Tyrode's solution which consisted of (in mM): 140 NaCl, 5.4 KCl, 1.2 KH_2PO_4, 1.0 $MgCl_2$, 1.8 $CaCl_2$, 5.5 glucose, and 5 HEPES, with pH adjusted to pH 7.4 with NaOH, at 35°C. The right atrial appendage was pinned open and cut into 8-10 strips. The strips were transferred from the Tyrode's solution to a low Ca^{2+}, Mg^{2+} free solution containing (in mM): 140 NaCl, 5.4 KCl, 1.2 KH_2PO4, 0.2 $CaCl_2$, 50 taurine, 18.5 glucose, 5 HEPES, and 1 mg/ml BSA, with pH adjusted to 6.9 with NaOH. The tissue was washed in this solution by gentle inversion and subsequent transfers between three separate round-bottom tubes. Following the washing procedure, the atrial strips were transferred into 5 ml of low Ca^{2+}, Mg^{2+} free solution containing 3.2 mg of collagenase (type II, Worthington; 335 U/mg), 75 µl of elastase (Worthington; 4.84 U/mgP), and 65.2 µl of 1 mg/100 µl protease solution from *Streptomyces griseus* (type XIV, Sigma-Aldrich; 4.3 U/mg). Enzymatic digestion took place for 30 min at 35ºC with manual agitation of the tube every 5 minutes. The tissue was then transferred to 2.5 ml of modified Kraft-Brühe (KB) buffer solution containing (in mM): 100 K-glutamate, 10 K-aspartate, 25 KCl, 10 KH_2PO_4, 2 $MgSO_4$, 20 taurine, 5 creatine, 0.5 EGTA, 20 glucose and 5 HEPES, and 1% BSA, with pH adjusted to 7.2 with KOH. The tissue was washed in this solution by gentle inversion and subsequent transfers between three separate round-bottom tubes. The tissue strips were transferred to a final round bottom tube containing 2.5 ml of modified KB solution and left to rest for 5 min before the strips were mechanically triturated for 7.5 min at 35°C with a wide-bore pipette. Approximately 5-7 ml of additional KB solution was added to the tube containing

the tissue and was placed at room temperature for one hour before electrophysiological experiments were performed.

2.3 Solutions & Pharmacology

2.3.1 Experimental Drugs

ANP (1-28) (mouse, rabbit, rat; Bachem) was obtained as a trifluroacetate salt and was dissolved in double distilled water (DD-H_20) to produce a 10 μM stock solution, which was stored at -80°C in 250 μl aliquots until time of use, at which point 250 μl aliquots were dissolved in 25 ml of external bath solution to yield the desired final experimental concentration of 100 nM. This solution was superfused through the recording chamber at room temperature.

mANP (H-SLRRSSCFGGRMDRIGAQSGLGCNSFRYRITAREDKQGWA-OH) (custom synthetic; Bachem) was obtained as an oxidized acetate salt and was dissolved in DD-H_2O to produce a 10 μM stock solution, which was stored at -80ºC in 250 μL aliquots. At time of use the 250 μL aliquots were dissolved in 25 mL of external bath solution to yield a final concentration of 100 nM. This solution was superfused through the recording chamber at room temperature (21°- 23°C).

Isoproterenol hydrochloride (Sigma-Aldrich) was used as a non-selective β-AR agonist in order to activate AC activity and increase intracellular cAMP levels. An initial 1 mM stock was prepared and subsequently diluted to produce a final stock concentration of 10 μM. The final stock was prepared fresh every hour and 25 μl of the stock solution was added to 25 ml of external bath solution to produce a final experimental concentration of 10 nM.

A71915 (Bachem) is a well-characterized NPR-A specific antagonist (Delporte *et al*, 1992). A71915 was used to examine the role of NPR-A in mediating the electrophysiological effects of ANP and mANP. A71915 was dissolved in DD-H_2O and separated into 100 µl aliquots. The aliquots were dissolved in 25 ml of external bath solution for a final experimental concentration of 500 nM.

2.3.2 Action Potential Solutions

AP external recording solution was normal Tyrode's solution and consisted of (in mM): 140 NaCl, 5.4 KCl, 1 $CaCl_2$, 1 $MgCl_2$, 10 HEPES, 5.5 Glucose, and buffered to a pH of 7.4 with NaOH. Internal pipette solution consisted of (in mM): 140 KCl, 5 NaCl, 0.2 $CaCl_2$, 5 EGTA, 4 K-ATP, 1 $MgCl_2$, 10 HEPES, 6.6 Na-phosphocreatine, 0.3 Na-GTP, and buffered to a pH of 7.2 with KOH. The internal solution was filtered through a 0.22 micron filter prior to use. Amphotericin-B was used to achieve the perforated patch clamp configuration. Amphotericin-B was dissolved in DMSO to make a final stock concentration of 20 mg/ml. Next, 10 µl of amphotericin stock solution was added to 0.5 ml of the AP internal solution to create a final concentration of 200 µg/ml of amphotericin-B. All solutions were well vortexed prior to use, and a fresh stock was made every hour throughout the experiment.

2.3.3 Calcium Current Solutions

The external calcium current recording solution consisted of (in mM): 140 CsCl, 5.4 TEA-Cl, 2 $CaCl_2$, 1 $MgCl_2$, 10 HEPES, 1 Glucose, and buffered to a pH of 7.4 with CsOH. The internal calcium current recording solution consisted of (in mM): 135 CsCl, 5

NaCl, 0.2 $CaCl_2$, 5 EGTA, 4 Mg-ATP, 1 $MgCl_2$, 10 HEPES, 6.6 Na-phosphocreatine, 0.3 Na-GTP, and buffered to a pH of 7.2 with CsOH. Lidocaine (0.3 M) was also added to block sodium current. The internal solution was filtered through a 0.22 micron filter prior to use.

2.4 Electrophysiological Protocols

Micropipettes were pulled from borosilicate glass (with filament, 1.5 mm OD, 0.86 mm ID; Sutter Instrument, Novato, CA) using a Flaming/Brown pipette puller (model P-97, Sutter Instrument). The resistance of these pipettes was 2-7 MΩ when filled with recording solution. Microelectrodes were positioned with a piezoelectric micromanipulator (Burleigh® Instruments, Burleigh TS-5000-150) mounted on the stage of an inverted microscope (Nikon Eclipse TE300). Seal resistances were 1–10 GΩ.

2.4.1 Action Potential Recordings

The perforated patch clamp technique was used for AP recordings in single right atrial myocytes (Rae *et al*, 1991). An aliquot of cell suspension was allowed to settle for 10 minutes in a 35 mm petri dish that was mounted on the stage of the microscope. The recording chamber was then superfused with Tyrode's solution and amphotericin-B was added to the pipette solution as described above (chapter 2.3.2). Gigaseals were achieved and access resistance was monitored for the appearance of capacitive transients. Access resistances of less than 30 M Ω were seen 10 to 15 minutes within sealing at which time APs were recorded in current clamp mode.

APs were elicited from atrial myocytes by applying a 20 ms depolarizing stimulus (0.03-0.1 nA) every 5 seconds using the Axopatch 200B amplifier (Molecular Devices). Using this protocol, APs were recorded over approximately 15 minute periods, during which the experiment took place and drugs were applied.

2.4.2 Calcium Current Recordings

The whole cell configuration of the patch-clamp technique was used for Ca^{2+} recordings in single right atrial myocytes (Hamill *et al*, 1981). The cell suspension was superfused with the external calcium containing solution (with drugs applied as needed) and pipettes were filled with the internal calcium recording solutions as described above (chapter 2.3.3).

To record $I_{Ca,L}$ during voltage clamp experiments the sarcolemma was ruptured and an access resistance between 5-20 MΩ was achieved. The series resistance was compensated by 80% using the Axopatch 200B amplifier (Molecular Devices).

Time course $I_{Ca,L}$ experiments were recorded by first applying a depolarizing voltage-clamp step from a -80 mV holding potential to -60 mV for 200 ms. Immediately after this pre-pulse, a 250 ms voltage-clamp step was applied from -60 mV to 0 mV.

Current-voltage (IV) relationships for $I_{Ca,L}$ were measured by applying a series of 250 ms steps in 10 mV increments at voltages between -60 mV to +60 mV from a holding potential of -80 mV. $I_{Ca,L}$ activation kinetics were determined by calculating chord conductance from the $I_{Ca,L}$ recordings using the equation: $G = (I/V_m - V_{rev})$; where G is the conductance, I is the current measured, V_m is the depolarizing voltage and V_{rev} is the apparent reversal potential. Peak conductance density was fit to a multi-component

Boltzmann function to produce a sigmoidal curve in order to calculate maximum conductance (G_{max}), the voltage at which 50% activation occurs ($V_{1/2}$), and the slope factor (k) from the equation:

$$y = \frac{A_1 - A_2}{1 + e^{(x - x_0 / dx)}} + A_2$$

$A_i = G$, $A_2 = G_{max}$, $x = V_m$, $x_0 = V_{1/2(act)}$ and dx = slope factor (k)

2.5 cAMP Assay

Right atrial myocytes were isolated as described (chapter 2.2). The entire sample of isolated cells in KB was centrifuged at 2000 rpm for 5 minutes. The supernatant was removed and the pellet was resuspended in external calcium current recording solution (described in chapter 2.4.3) in order to keep the conditions consistent with those during $I_{Ca,L}$ measurements. A hemocytometer was used to determine myocyte density. Cells were treated in six test conditions; control, ANP alone, mANP alone, ISO, ISO+ANP and ISO+mANP, and incubated for 15 minutes at 4ºC. Intracellular cAMP concentrations were determined using a HTRF® cAMP Femto2 kit (Cisbio US, Inc., Bedford, MA, US) according to manufacturer's instructions.

2.6 Statistical Analysis

Summary data are presented as means±SEM. The data were analyzed using a Repeated measures One-Way ANOVA followed by Tukey post-hoc analysis or paired Student's t-test, as appropriate, to identify significant differences (Sigma Stat 2.0 statistical analysis software (Jandel Scientific)). For cAMP assay analysis, standard

curves were fit and interpolated using Prism 6 (GraphPad software). In all cases $P < 0.05$ was considered significant.

CHAPTER 3: RESULTS

3.1 Effects of ANP on action potential morphology and L-type calcium current in right atrial myocytes in basal conditions

The first set of experiments in this study investigated the effects of ANP (100 nM) on AP morphology in isolated mouse right atrial myocytes in basal conditions (Fig. 3.1). The AP parameters measured included the resting membrane potential (RMP), AP upstroke velocity (V_{max}), AP overshoot, and action potential duration at 50, 70 and 90% repolarization (APD_{50}, APD_{70} and APD_{90}) (Table 1). RMP was -77.9±0.3 mV in control conditions and -77.9±0.3 mV after application of ANP (*P*=0.990). V_{max} was 150.0±7.1 V/s in control conditions and 149.3±7.1 V/s in the presence of ANP (*P*=0.989). AP overshoot was 60.3±6.6 mV in control conditions and 60.1±6.8 mV in the presence of ANP (*P*=0.937). APD_{50} was 12.4±2.0 ms in control conditions and 12.56±1.9 ms in the presence of ANP (*P*=0.948). APD_{70} was 24.6±3.3 ms in control conditions and 24.6±3.2 ms in the presence of ANP (*P*=0.993). APD_{90} was 55.8±4.5 ms in control conditions and 55.5±4.3 ms in the presence of ANP (*P*=0.818). Collectively, these analyses demonstrate that ANP had no significant effect on atrial AP morphology in basal conditions.

Previous studies in our laboratory have identified $I_{Ca,L}$ as a major target of regulation by NPs in the heart (Springer *et al*., 2012). Thus, despite the lack of effect of ANP on atrial AP morphology, the effects of ANP on atrial $I_{Ca,L}$ were also measured in basal conditions (Fig. 3.2). Figure 3.2A illustrates representative $I_{Ca,L}$ recordings during a voltage clamp step to 0 mV (holding potential was -60 mV) in control conditions and following application of ANP (100 nM).

Figure 3.1: Effects of ANP on right atrial myocyte action potential morphology in basal conditions. (A) Representative stimulated atrial myocyte APs in control conditions and following application of ANP (100 nm). (B) Summary of the effects of ANP on right atrial AP duration in basal conditions. Dashed line represents ANP had no effect on the AP morphology in basal conditions (n=6 myocytes; analyzed by paired Student's t-test). See Table 1 for additional analysis.

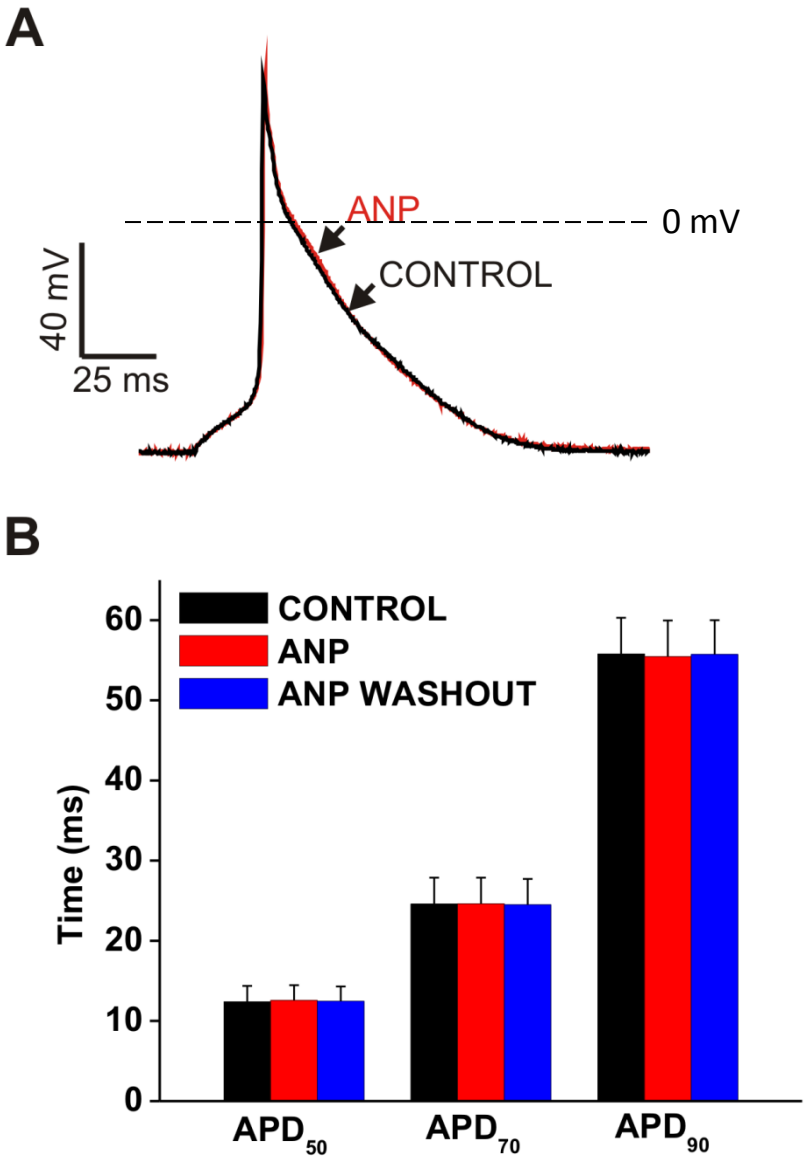
A
ANP
0 mV
CONTROL
40 mV
25 ms
B
CONTROL
ANP
ANP WASHOUT
Time (ms)
60
50
40
30
20
10
0
APD50
APD70
APD90

Figure 3.1

Table 1: Summary of action potential parameters following application of ANP (100 nM) in basal conditions in right atrial myocytes.

	Control	ANP
RMP (mV)	-77.9±0.3	-78.0±0.3
V_{max} (V/s)	150.0±7.1	149.3±7.1
Overshoot (mV)	60.3±6.6	60.1±6.8
APD_{50} (ms)	12.4±2.0	12.6±1.9
APD_{70} (ms)	24.6±3.3	24.6±3.2
APD_{90} (ms)	55.8±4.5	55.5±4.3

Data are means ± SEM; *n*=6 right atrial myocytes. ANP had no effect on the AP parameters (analyzed by paired Students t-test).

Figure 3.2: Effects of ANP on right atrial myocyte L-type Ca^{2+} current ($I_{Ca,L}$) in basal conditions. (A) Representative right atrial $I_{Ca,L}$ recordings in control conditions and following application of ANP (100 nM). The voltage clamp protocol used (inset) allows measurement of Cav1.2 and Cav1.3 dependent $I_{Ca,L}$ (see methods). (B) Summary I-V relationships for the effects of ANP on right atrial myocyte $I_{Ca,L.}$ (C) Summary $I_{Ca,L}$ conductance density plots demonstrating the effects of ANP on $I_{Ca,L}$ activation kinetics (see Table 2 for additional analysis of $I_{Ca,L}$ kinetics). ANP had no effect on $I_{Ca,L}$ in isolated atrial myocytes in basal conditions (*n*=7 right atrial myocytes; analyzed by paired Student's t-test).

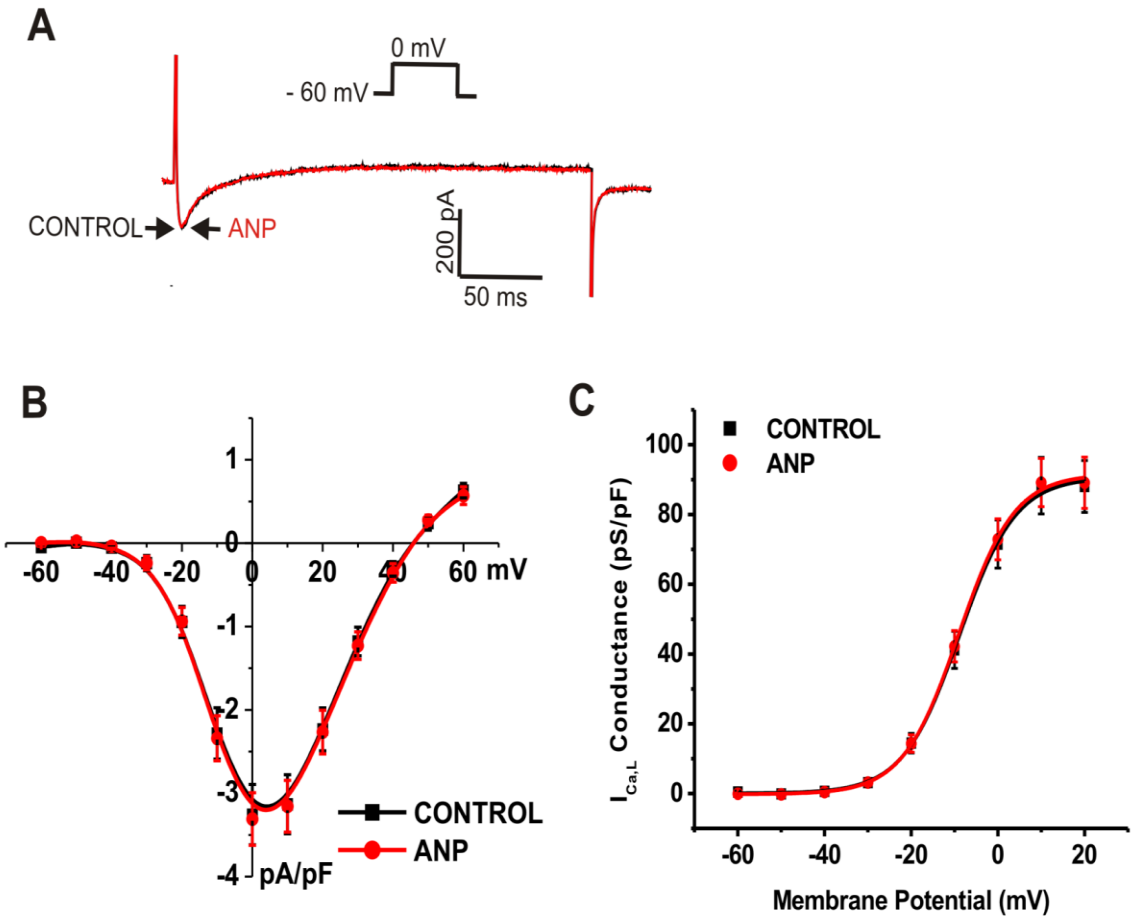
A
0 mV
- 60 mV
CONTROL
ANP
200 pA
50 ms
B
1
0
-1
-2
-3
-4
-60
-40
-20
0
20
40
60 mV
pA/pF
CONTROL
ANP
C
CONTROL
ANP
100
80
60
40
20
0
$I_{Ca,L}$ Conductance (pS/pF)
-60
-40
-20
0
20
Membrane Potential (mV)

Figure 3.2

The effect of ANP on $I_{Ca,L}$ was quantified in a summary current-voltage (IV) relationship (Fig 3.2B). Consistent with the representative recordings, the $I_{Ca,L}$ IV relationship showed no change upon application of ANP (P=0.960). Figure 3.2C shows the effects of ANP on $I_{Ca,L}$ activation kinetics in basal conditions. Maximum conductance (G_{max}), the voltage required for 50% channel activation ($V_{1/2(act)}$) and the activation curve slope constant (k) were measured from Boltzman fits of chord conductance data (Table 2). There was no significant difference in the conductance analysis parameters upon application of ANP. G_{max} was 90.7±1.3 pS/pF in control conditions and 91.6±1.2 pS/pF in the presence of ANP (P=0.926). $V_{1/2(act)}$ was -8.9±0.4 mV in control conditions and -9.1±0.4 mV upon application of ANP (P=0.838). Finally, k was 6.5±0.4 in control and 6.4±0.3 with ANP (P=0.627). These data demonstrate that in basal conditions ANP has no effect on $I_{Ca,L}$ in right atrial myocytes.

3.2 Effects of mANP on action potential morphology and L-type calcium current in right atrial myocytes in basal conditions

In order to begin unraveling the effects of mANP on atrial electrophysiology, APs were recorded in isolated right atrial myocytes in basal conditions and after application of mANP (100 nM) (Fig. 3.3; Table 3). RMP was -77.4±0.4 mV in control conditions and -77.8±0.3 mV after mANP application (P=0.882). V_{max} was 144.2±5.3 V/s in control conditions and 143.8±5.0 V/s in the presence of mANP (P=0.961). AP overshoot was 60.8±3.9 mV in control conditions and 59.8±3.5 mV in the presence of mANP (P=0.860). APD_{50} was 15.2±0.8 ms in control conditions and 15.6±0.6 ms in the presence of mANP

Table 2: Summary of $I_{Ca,L}$ steady state conductance analysis following application of ANP (100 nM) in basal conditions in right atrial myocytes.

	Control	**ANP**
G_{max} (pS/pF)	90.7±1.3	91.6±1.2
$V_{1/2(act)}$ (mV)	-8.9±0.4	-9.1±0.4
k	6.5±0.4	6.4±0.3

Data are means ± SEM. ANP had no effect on $I_{Ca,L}$ steady state conductance parameters (*n*=7 right atrial myocytes; analyzed by paired Student's *t*-test).

Figure 3.3: Effects of mANP on right atrial myocyte action potential morphology in basal conditions. (A) Representative stimulated atrial myocyte APs in control conditions and following application of mANP (100 nM). (B) Summary of the effects of mANP on right atrial AP duration in basal conditions. mANP had no effect on the AP morphology in basal conditions (*n*=5 myocytes; analyzed by paired Student's t-test). See Table 3 for additional analysis.

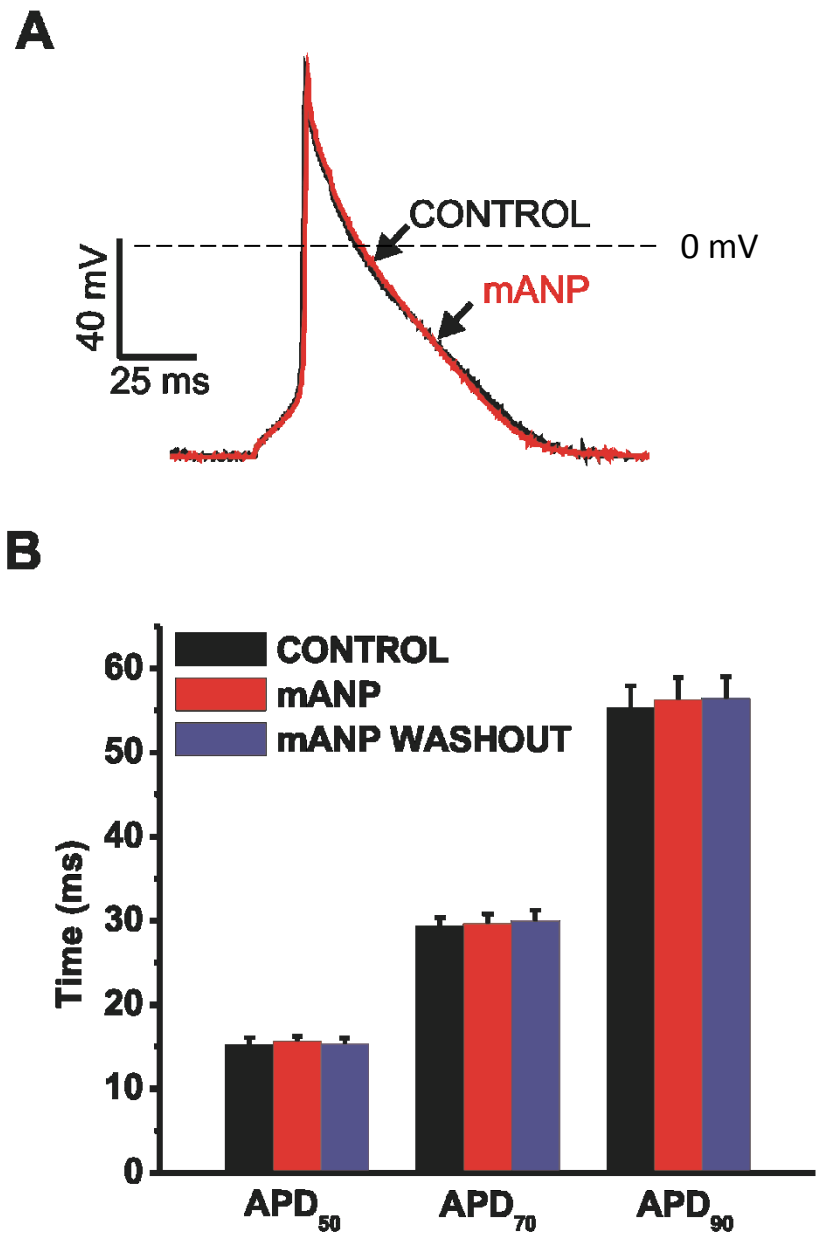
A
CONTROL
0 mV
mANP
40 mV
25 ms
B
CONTROL
mANP
mANP WASHOUT
Time (ms)
60
50
40
30
20
10
0
APD50
APD70
APD90

Figure 3.3

Table 3: Summary of action potential parameters following application of mANP (100 nM) in basal conditions in right atrial myocytes.

	Control	**mANP**
RMP (mV)	-77.4±0.4	-77.8±0.3
V_{max} (V/s)	144.2±5.3	143.8±5.0
Overshoot (mV)	60.8±3.9	59.8±3.5
APD_{50} (ms)	15.2±0.8	15.6±0.6
APD_{70} (ms)	29.3±1.1	29.6±1.2
APD_{90} (ms)	55.3±2.7	56.3±2.7

Data are means ± SEM. mANP had no effect on the AP parameters (*n*=5 right atrial myocytes; analyzed by paired Students t-test).

(P=1.000). APD_{70} was 29.3±1.1 ms in control conditions and 29.6±1.2 ms in the presence of mANP (P=0.690). APD_{90} was 55.3±2.7 ms in control conditions and 56.3±2.7 ms in the presence of mANP (P=0.793). Thus, application of mANP in basal conditions had no significant effect on any AP parameters measured (n=5 right atrial myocytes).

The effects of mANP on right atrial $I_{Ca,L}$ in basal condition were also studied (Fig. 3.4). Figure 3.4A illustrates representative $I_{Ca,L}$ recordings during a voltage clamp step to 0 mV (holding potential was -60 mV) in control conditions and following application of mANP (100 nM). The effect of mANP on $I_{Ca,L}$ was quantified in summary current-voltage (IV) relationships (Fig 3.4B). Consistent with the representative recordings, the $I_{Ca,L}$ IV relationship showed no change upon application of mANP (P=0.982). Figure 3.4C shows $I_{Ca,L}$ conductance density plots in basal conditions and after application of mANP. I_{CaL} G_{max}, $V_{1/2(act)}$ and k were measured from Boltzman fits of chord conductance data (Table 4). G_{max} was 101.8±2.9 pS/pF in control conditions and 112.0±1.5 pS/pF in the presence of mANP (P=0.222). $V_{1/2(act)}$ was -10.9±0.9 mV in control conditions and -11.1±0.4 mV upon application of mANP (P=0.639). Finally k was 7.9±0.8 in control and 8.4±0.4 with mANP (P=0.489). Thus, there was no significant effect of mANP on $I_{Ca,L}$ activation kinetics in right atrial myocytes in basal conditions. Collectively, these data demonstrate that mANP has no effect on $I_{Ca,L}$ in right atrial myocytes in basal conditions.

Figure 3.4: Effects of mANP on right atrial myocyte L-type Ca^{2+} current ($I_{Ca,L}$) in basal conditions. (A) Representative right atrial $I_{Ca,L}$ recordings in control conditions and following application of mANP (100 nM). The voltage clamp protocol used (inset) allows measurement of Cav1.2 and Cav1.3 dependent $I_{Ca,L}$ (see methods). (B) Summary I-V relationships for the effects of mANP on right atrial myocyte $I_{Ca,L.}$ (C) Summary $I_{Ca,L}$ conductance density plots demonstrating the effects of mANP on $I_{Ca,L}$ activation kinetics (see Table 4 for additional analysis of $I_{Ca,L}$ kinetics). mANP had no effect on $I_{Ca,L}$ in isolated atrial myocytes in basal conditions (*n*=5 right atrial myocytes; analyzed by paired Student's t-test).

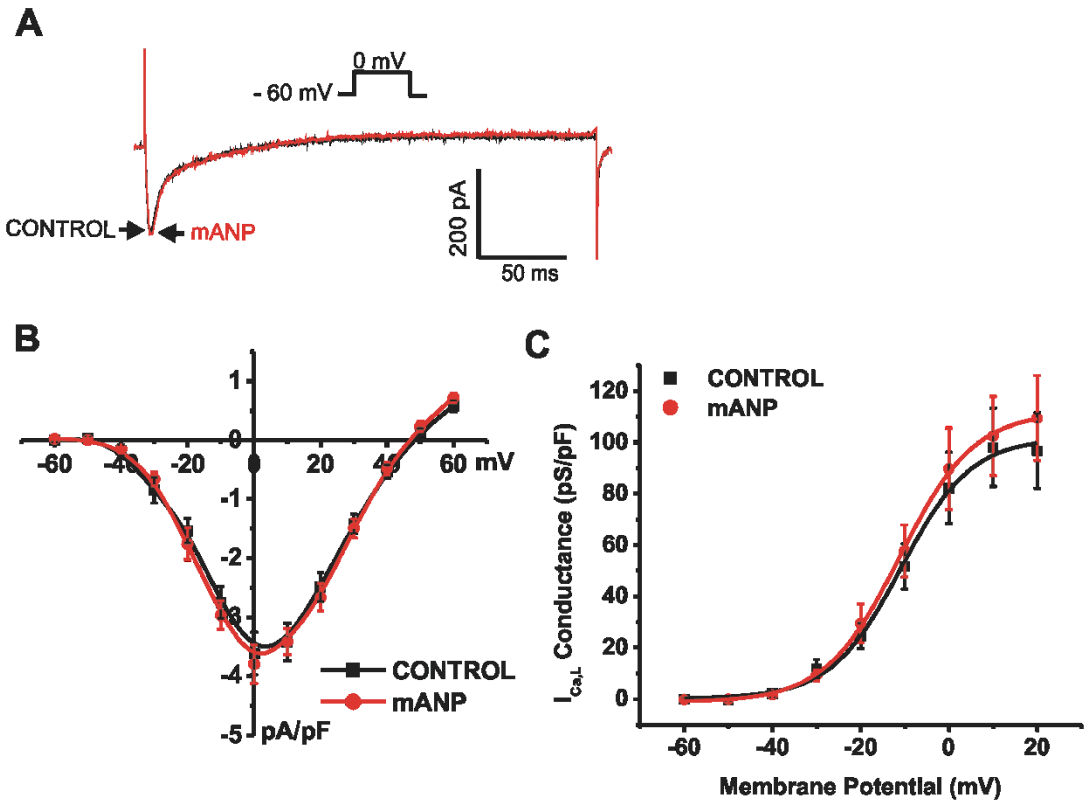
A
0 mV
- 60 mV
CONTROL
mANP
200 pA
50 ms
B
1
0
-1
-2
-3
-4
-5
-60
-20
20
60 mV
CONTROL
mANP
pA/pF
C
CONTROL
mANP
120
100
80
60
40
20
0
-60
-40
-20
0
20
Membrane Potential (mV)
Conductance (pS/pF)

Figure 3.4

Table 4: Summary of $I_{Ca,L}$ steady state conductance analysis following application of mANP (100 nM).

	Control	**mANP**
G_{max} (pS/pF)	101.8±2.9	112.0±1.5
$V_{1/2(act)}$ (mV)	-10.9±0.9	-11.1±0.4
k	7.9±0.8	8.4±0.4

Data are means ± SEM. mANP had no effects on $I_{Ca,L}$ steady state conductance parameters (*n*=5 right atrial myocytes; analyzed by paired Student's t-test).

3.3 Effects of ANP on L-type calcium current in right atrial myocytes in the presence of isoproterenol

Previous work in our laboratory has shown that BNP (Springer *et al*., 2012) and CNP (Rose *et al*., 2003) have robust effects on L-type Ca^{2+} current in atrial myocytes in the presence of β-AR stimulation. Therefore, the effects of ANP (100 nM) on $I_{Ca,L}$ were next studied in the presence of the β-AR agonist isoproterenol (ISO; 10 nM) (Fig. 3.5). Figure 3.5A illustrates representative $I_{Ca,L}$ recordings during a voltage clamp step to 0 mV (holding potential was -60 mV) in control conditions, in the presence of ISO and following application of ANP in the presence of ISO. These recordings and the representative time course (Figure 3.5B) demonstrate that peak $I_{Ca,L}$ was increased following application of ISO in right atrial myocytes. Peak $I_{Ca,L}$ was further increased upon application of ANP (in the presence of ISO). These effects of ISO and ANP were fully reversible when washed out.

The effects of ISO and ANP on $I_{Ca,L}$ were quantified in summary IV relationships (Figure 3.5C). In agreement with the representative recordings and time course data, the IV relations showed a significant increase in $I_{Ca,L}$ density upon application of ISO between the voltages of -30 mV and +30 mV ($P<0.05$). Application of ANP in the presence of ISO caused a further increase in $I_{Ca,L}$ ($P<0.05$) between the voltages of -30 mV and 0 mV. Figure 3.5D shows $I_{Ca,L}$ conductance analysis between the three conditions. G_{max}, $V_{1/2(act)}$ and k were measured from Boltzman fits of chord conductance data (Table 5). Analysis showed a significant increase in G_{max} from 79.3±0.3 pS/pF in control conditions to 168.1±2.3 pS/pF in the presence of ISO ($P<0.05$). G_{max} was

Figure 3.5: Effects of ANP on $I_{Ca,L}$ in right atrial myocytes in the presence of the β-adrenergic receptor agonist isoproterenol (ISO). (A) Representative right atrial $I_{Ca,L}$ recordings in control conditions, in the presence of ISO (10 nM) and following application of ISO + ANP (100 nM). (B) Time course of the effects of ISO and ANP on peak atrial $I_{Ca,L}$ (C) Summary I-V relationships for right atrial myocyte $I_{Ca,L}$ in control conditions, in the presence of ISO and following application of ISO + ANP. (D) Summary $I_{Ca,L}$ conductance density plots demonstrating the effects of ISO and ANP on right atrial $I_{Ca,L}$ activation kinetics (see Table 5 for additional analysis). *n*=8 right atrial myocytes; **P*<0.05 vs. control; †*P*<0.05 vs. ISO by one-way ANOVA with a Tukey posthoc test.

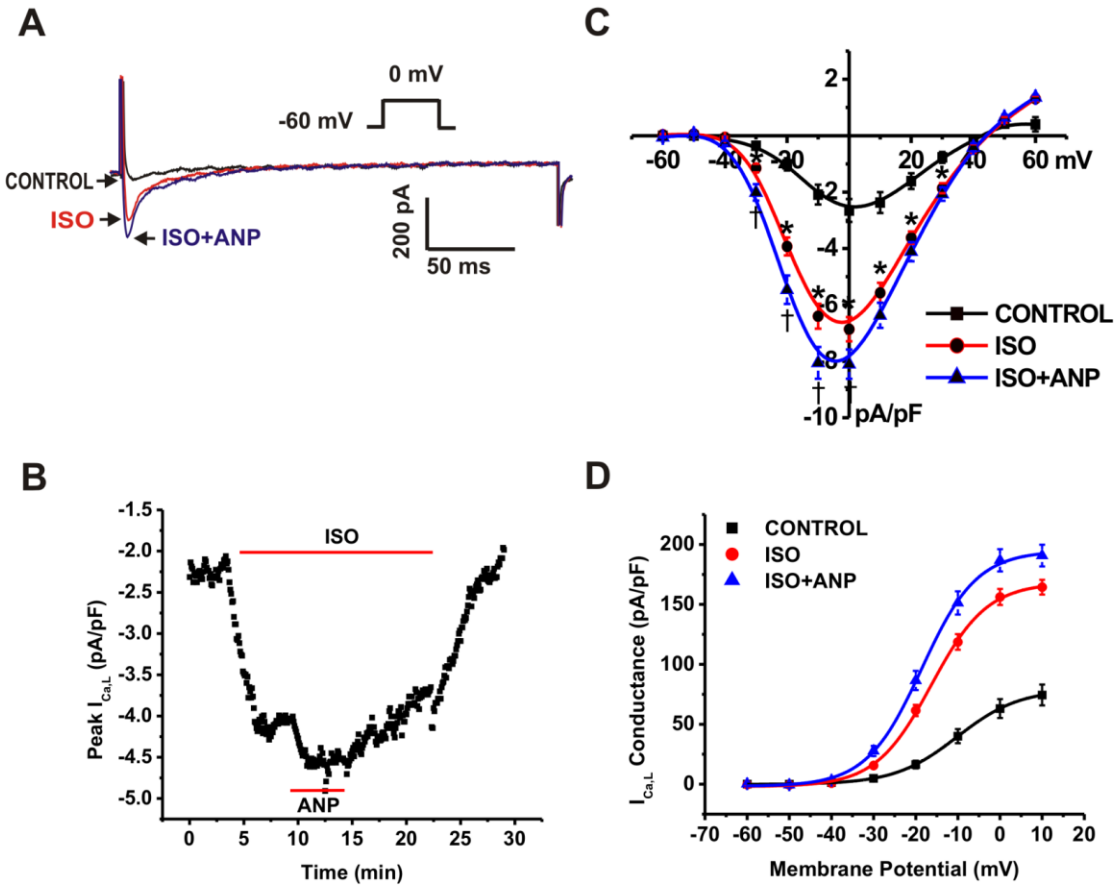
A
0 mV
-60 mV
CONTROL
ISO
ISO+ANP
200 pA
50 ms
C
2
-2
-4
-6
-8
-10
pA/pF
-60
-40
-20
20
40
60 mV
CONTROL
ISO
ISO+ANP
B
Peak $I_{Ca,L}$ (pA/pF)
-1.5
-2.0
-2.5
-3.0
-3.5
-4.0
-4.5
-5.0
ISO
ANP
0
5
10
15
20
25
30
Time (min)
D
CONTROL
ISO
ISO+ANP
$I_{Ca,L}$ Conductance (pA/pF)
200
150
100
50
0
-70
-60
-50
-40
-30
-20
-10
0
10
20
Membrane Potential (mV)

Figure 3.5

Table 5: Summary of $I_{Ca,L}$ steady state conductance analysis following application of ISO (10 nM) and ANP (100 nM) in right atrial myocytes.

	Control	**ISO**	**ISO+ANP**
G_{max} (pS/pF)	79.3±0.3	168.05±2.3*	194.7±2.4*†
$V_{1/2(act)}$ (mV)	-10.2±0.1	-16.3±0.4*	-18.6±0.4*†
K	7.4±0.1	6.6±0.3	6.5±0.3

Data are means ± SEM; *n*=8 right atrial myocytes. **P*<0.05 vs. control; †*P*<0.05 vs. ISO by one-way ANOVA with a Tukey posthoc test.

further increased to 194.7±2.4 pS/pF upon application of ANP (P<0.05). $V_{1/2(act)}$ was also significantly hyperpolarized from -10.2±0.1 mV in control conditions to -16.3±0.4 mV upon application of ISO (P<0.05). $V_{1/2(act)}$ was further hyperpolarized to -18.6±0.4 mV after ANP application (P<0.05). Finally there was no significant difference in the slope factor (k) between the 3 experimental groups; k was 7.4±0.1 in control, 6.6±0.3 in the presence of ISO, and 6.5±0.3 with ANP (P=0.269).

3.4 Effect of mANP on L-type calcium current in right atrial myocytes in the presence of isoproterenol

Next, the effects of mANP (100 nM) on $I_{Ca,L}$ were studied in the presence of ISO (10 nM; Fig. 3.6). Figure 3.6A illustrates representative $I_{Ca,L}$ recordings during a voltage clamp step to 0 mV (holding potential was -60 mV) in control conditions, in the presence of ISO and following application of mANP. These recordings and the representative time course (Fig 3.6B) demonstrate that peak $I_{Ca,L}$ was increased upon application of ISO in right atrial myocytes. In complete contrast to ANP, peak $I_{Ca,L}$ was decreased upon application of mANP in the presence of ISO. The effects of ISO and mANP were fully reversible when washed out.

The effects of ISO and mANP on $I_{Ca,L}$ were quantified in a summary IV relationship (Fig. 3.6C). Consistent with the representative recordings and time course, the $I_{Ca,L}$ IV relation showed a significant increase in $I_{Ca,L}$ density upon application of ISO between the voltages -30 mV and +40 mV (P<0.05). Application of mANP in the presence of ISO caused a decrease in $I_{Ca,L}$ (P<0.05) between the voltages of -30 mV and 0 mV. Figure 3.6D shows steady state conductance analysis between the three conditions. G_{max}, $V_{1/2(act)}$

Figure 3.6: Effects of mANP on $I_{Ca,L}$ in right atrial myocytes in the presence of the β-adrenergic receptor agonist isoproterenol (ISO). (A) Representative right atrial $I_{Ca,L}$ recordings in control conditions, in the presence of ISO (10 nM) and following application of ISO + mANP (100 nM). (B) Time course of the effects of ISO + mANP on peak atrial $I_{Ca,L}$ (C) Summary I-V relationships for right atrial myocyte $I_{Ca,L}$ in control conditions, in the presence of ISO and following application of ISO + mANP. (D) Summary $I_{Ca,L}$ conductance density plots demonstrating the effects of ISO and mANP on right atrial $I_{Ca,L}$ activation kinetics (see Table 6 for additional analysis). *n*=6 right atrial myocytes; **P*<0.05 vs. control; †*P*<0.05 vs. ISO by one-way ANOVA with a Tukey posthoc test.

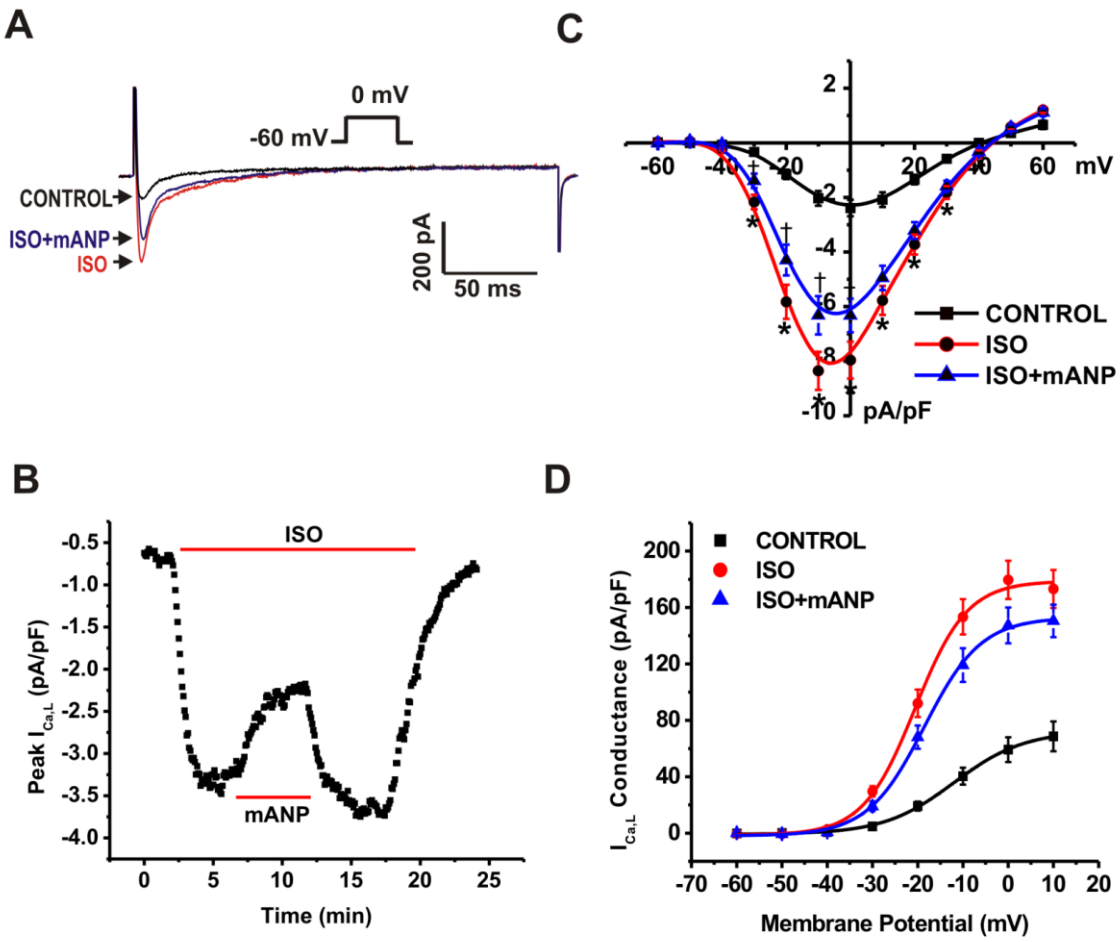
A
0 mV
-60 mV
CONTROL
ISO+mANP
ISO
200 pA
50 ms
C
2
-2
-4
-6
-8
-10
pA/pF
-60
-40
-20
20
40
60
mV
CONTROL
ISO
ISO+mANP
B
ISO
mANP
Peak $I_{Ca,L}$ (pA/pF)
-0.5
-1.0
-1.5
-2.0
-2.5
-3.0
-3.5
-4.0
0
5
10
15
20
25
Time (min)
D
CONTROL
ISO
ISO+mANP
$I_{Ca,L}$ Conductance (pA/pF)
200
160
120
80
40
0
-70
-60
-50
-40
-30
-20
-10
0
10
20
Membrane Potential (mV)

Figure 3.6

Table 6: Summary of $I_{Ca,L}$ steady state conductance analysis following application of ISO (10 nM) and mANP (100 nM) in right atrial myocytes.

	Control	**ISO**	**ISO+mANP**
G_{max} (pS/pF)	72.5±1.3	178.2±3.3*	152.9±2.2*†
$V_{1/2(act)}$ (mV)	-12.0±0.2	-20.6±0.6*	-18.5±0.4*†
k	7.8±0.4	5.7±0.5	6.3±0.4

Data are means ± SEM; *n*=6 right atrial myocytes. **P*<0.05 vs. control; †*P*<0.05 vs. ISO by one-way ANOVA with a Tukey posthoc test.

and k were measured from Boltzman fits of chord conductance data (Table 6). Analysis showed a significant increase in G_{max} from 72.5±1.3 pS/pF in control conditions to 178.8±3.3 pS/pF in the presence of ISO (P<0.05). G_{max} significantly decreased to 152.9±2.2 pS/pF upon application of mANP (P<0.05). $V_{1/2(act)}$ was also hyperpolarized from -12.0±0.4 mV in control conditions to -20.6±0.6 mV upon application of ISO (P<0.05). In contrast to ANP, $V_{1/2(act)}$ was significantly depolarized after mANP application (-18.5±0.4 mV; P<0.05). Finally there was no significant difference in the slope factor, k, between the 3 experimental groups; k was 7.8±0.4 in control, 5.8±0.5 in the presence of ISO, and 6.3±0.4 with ANP (P=0.193).

3.5 Effects of ANP and mANP on L-type calcium current in NPR-C$^{-/-}$ right atrial myocytes

Our previous work has shown that NPs can either increase or decrease $I_{Ca,L}$ depending on which NPRs are activated in different experimental conditions (Rose *et* al., 2003; Rose *et al*., 2004; Springer *et al*., 2012). In order to evaluate the role of NPR-C signalling in mediating the effects of ANP and mANP, $I_{Ca,L}$ was measured in atrial myocytes isolated from NPR-C$^{-/-}$ mice (Fig. 3.7). Figure 3.7A illustrates representative $I_{Ca,L}$ recordings during a voltage clamp step to 0 mV (holding potential was -60 mV) in control conditions, in the presence of ISO (10 nM) and following application of ANP (100 nM). These recordings and the representative time course (Fig. 3.7B) demonstrate peak $I_{Ca,L}$ was increased following application of ISO and peak $I_{Ca,L}$ was further increased upon application of ANP in the presence of ISO. The effects of ISO and ANP were fully reversible when washed out. Summary data (Fig. 3.7C) shows a significant increase in

Figure 3.7: Effects of ANP and mANP on $I_{Ca,L}$ in the presence of ISO in right atrial myocytes isolated from mutant mice lacking functional NPR-C receptors (NPR-$C^{-/-}$). (A) Representative right atrial $I_{Ca,L}$ in control conditions, in the presence of ISO (10 nM) and following application of ISO + ANP (100 nM). (B) Time course of the effects of ISO and ANP on peak atrial $I_{Ca,L}$. (C) Summary of the effects of ISO + ANP on peak $I_{Ca,L}$ density (measured at 0mV) in NPR-$C^{-/-}$ mice (*n*=6 right atrial myocytes). (D) Representative right atrial $I_{Ca,L}$ in control conditions, in the presence of ISO and following application of ISO and mANP (100 nM). (E) Time course of the effects of ISO and mANP on peak atrial $I_{Ca,L}$. (F) Summary of the effects of ISO + mANP on peak $I_{Ca,L}$ density (measured at 0mV) in NPR-$C^{-/-}$ mice (*n*=9 right atrial myocytes). **P*<0.05 vs. control; †*P*<0.05 vs. ISO by one-way ANOVA with a Tukey posthoc test. Some data provided by RA Rose.

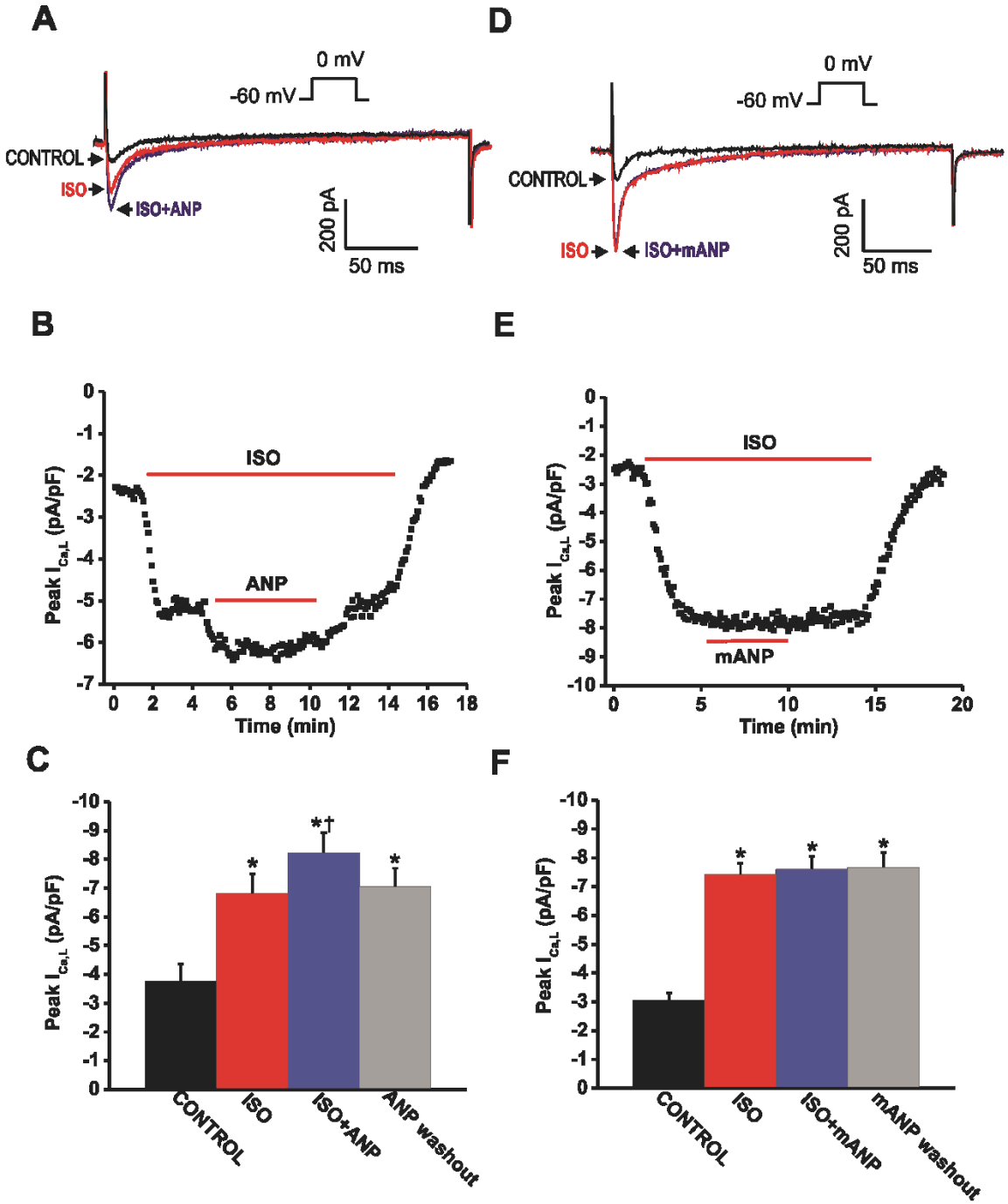
A
0 mV
-60 mV
CONTROL
ISO
ISO+ANP
200 pA
50 ms
D
0 mV
-60 mV
CONTROL
ISO
ISO+mANP
200 pA
50 ms
B
ISO
ANP
Peak $I_{Ca,L}$ (pA/pF)
Time (min)
E
ISO
mANP
Peak $I_{Ca,L}$ (pA/pF)
Time (min)
C
Peak $I_{Ca,L}$ (pA/pF)
CONTROL
ISO
ISO+ANP
ANP washout
F
Peak $I_{Ca,L}$ (pA/pF)
CONTROL
ISO
ISO+mANP
mANP washout

Figure 3.7

peak $I_{Ca,L}$ in the presence of ISO compared to the control condition (P<0.05). The addition of ANP further increased $I_{Ca,L}$ versus the ISO condition (P<0.05). These data demonstrate that ANP maintained its ability to increase $I_{Ca,L}$ in the presence of ISO in atrial myocytes isolated from NPR-$C^{-/-}$ mice indicating that the effects of ANP are not mediated by NPR-C. Next, the effects of mANP (100 nM) on $I_{Ca,L}$ were measured in NPR-$C^{-/-}$ atrial myocytes in the presence of ISO. Figure 3.7D illustrates representative $I_{Ca,L}$ recordings during a voltage clamp step to 0 mV (holding potential was -60 mV) in control conditions, in the presence of ISO (10 nM) and following application of mANP in the presence of ISO. These recordings and the representative time course (Fig. 3.7E) demonstrate that peak $I_{Ca,L}$ was increased following application of ISO. In contrast to ANP, mANP had no effect on peak $I_{Ca,L}$ (in the presence of ISO) in NPR-$C^{-/-}$ myocytes. Summary data (Fig. 3.7F) show a significant increase in peak $I_{Ca,L}$ in the presence of ISO compared to the control conditions (P<0.05). The addition of mANP had no effect on $I_{Ca,L}$ versus the ISO condition (P=0.989). These data demonstrate that mANP lost its ability to decrease $I_{Ca,L}$ in the presence of ISO in atrial myocytes isolated from NPR-$C^{-/-}$ mice. These data indicate that the effects of mANP are mediated by NPR-C.

3.6 Effect of ANP on L-type calcium current in right atrial myocytes in the presence of NPR-A blockade

The experiments presented above clearly demonstrate that the effects of ANP on $I_{Ca,L}$ are not dependent on NPR-C signalling. ANP can also bind and signal through NPR-A and we have recently demonstrated that related NPs (BNP and CNP) can increase atrial $I_{Ca,L}$ via the NPR-A/B receptors (Springer *et al*., 2012). Accordingly, the role of NPR-A

Figure 3.8: Effects of ISO + ANP on $I_{Ca,L}$ in right atrial myocytes in the presence of the NPR-A antagonist A71915. (A) Representative right atrial $I_{Ca,L}$ recordings in control conditions, in the presence of ISO (10 nM) and A71915 (500 nM) and following application of ANP (100 nM) in the presence of ISO and A71915. (B) Time course of the effects of ISO, A71915 and ANP on peak atrial $I_{Ca,L.}$ (C) Summary of the effects of ISO, A71915 and ANP on peak $I_{Ca,L}$ density (measured at 0 mV) in right atrial myocytes (n=5 right atrial myocytes). *P<0.05 vs. control by one-way ANOVA with a Tukey posthoc test. ANP had no effect (P=0.991) on atrial $I_{Ca,L}$ following NPR-A blockade.

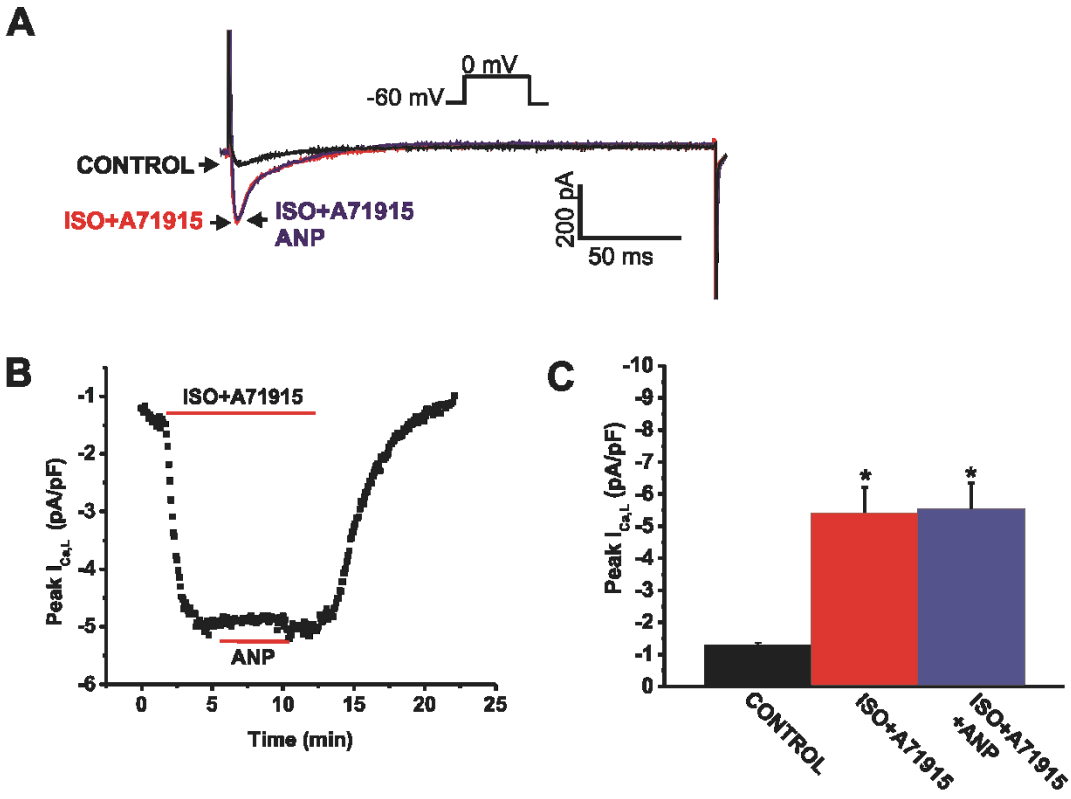
A
0 mV
-60 mV
CONTROL
ISO+A71915
ISO+A71915
ANP
200 pA
50 ms
B
ISO+A71915
ANP
Peak $I_{Ca,L}$ (pA/pF)
Time (min)
C
Peak $I_{Ca,L}$ (pA/pF)
CONTROL
ISO+A71915
ISO+A71915 +ANP

Figure 3.8

in mediating the effects of ANP on L-type calcium current was assessed using an NPR-A antagonist denoted A71915 (500 nM) (Delporte *et al*, 1992) (Fig. 3.8). Previous work in our laboratory showed that A71915 alone had no effect on $I_{Ca,L}$ (Springer *et al*., 2012), therefore in this study ISO and A71915 were applied together. Figure 3.8A illustrates representative $I_{Ca,L}$ recordings during a voltage clamp step to 0 mV (holding potential was -60 mV) in control conditions, in the presence of ISO + A71915 (10 nM) and following application of ANP in the presence of ISO and A71915. These recordings and the representative time course (Fig. 3.8B) demonstrate that in the presence of ISO + A71915, peak $I_{Ca,L}$ was increased in approximately 5 minutes in right atrial myocytes. Peak $I_{Ca,L}$ was not changed upon application of ANP for an additional 5 minutes. Summary data (Fig. 3.8C) shows a significant increase in peak $I_{Ca,L}$ in the presence of ISO + A71915 compared to the control condition ($P<0.05$). The addition of ANP had no effect on $I_{Ca,L}$ versus the ISO + A71915 condition ($P=0.991$). These data demonstrate that ANP lost its ability to increase atrial $I_{Ca,L}$ (in the presence of ISO) following NPR-A blockade with A71915. These data indicate that the effects of ANP are primarily mediated via NPR-A signalling.

3.7 Effects of ANP and mANP on intracellular cAMP production in right atrial myocytes

Our previous data has shown that NPs are able to effect $I_{Ca,L}$ via pathways that modulate cAMP levels (Azer *et al*., 2012; Rose *et al*., 2003; Springer *et al.,* 2012). Specifically, NPR-A is linked to a GC, which upon activation increases cGMP levels (Potter *et al*., 2006). Elevated cGMP inhibits PDE3 activity, which slows the degradation

of cAMP (Omori & Kotera *et al*., 2007; Zaccolo & Movesian *et al*., 2007). This results in an increase in cAMP and an increase in $I_{Ca,L}$ in atrial myocytes in the presence of BNP. In contrast, NPR-C is linked to G_i, which inhibits AC activity and, subsequently directly reduces cAMP concentration and decreases $I_{Ca,L}$ in cardiomyocytes. (Anand-Srivastava *et* al., 1993; Rose *et al*., 2003; Rose *et al*., 2004). Based on these prior findings, I hypothesized that ANP (acting via NPR-A) and mANP (acting via NPR-C) would have opposing effects on intracellular cAMP production. Accordingly, the effects of ANP and mANP on intracellular cAMP concentration were measured in the absence and presence of ISO in isolated right atrial myocytes (Fig. 3.9). Summary data (Fig. 3.9A) shows ANP had no effect on intracellular cAMP concentration in basal conditions (P=0.463). As expected, basal intracellular cAMP levels were increased upon application of ISO (10 nM) (P<0.05). Consistent with our electrophysiological data, cAMP levels were further increased following application of ANP (100 nM) in the presence of ISO (P<0.05) Summary data (Fig. 3.9B) shows mANP had no effect in basal conditions on intracellular cAMP concentration (P=0.445). Basal intracellular cAMP levels were increased upon application of ISO (10 nM) (P<0.05). Application of mANP (100 nM) in the presence of ISO resulted in a decrease in cAMP levels (P<0.05). cAMP concentration was standardized to 1000 cells. Thus, ANP and mANP did in fact elicit opposite effects on cAMP concentrations in atrial myocytes in the presence of ISO.

Figure 3.9: Effects of ANP and mANP on intracellular cAMP production in the absence and presence of ISO in right atrial myocytes. (A) Summary of the effects of ANP (100 nM), ISO (10 nM) and ISO+ANP on right atrial myocyte cAMP production. (B) Summary of the effects of mANP (100 nM), ISO and ISO+mANP on right atrial myocyte cAMP production. cAMP concentration was standardized to 1000 cells (n=6 right atrial myocyte isolations). *P<0.05 vs. control; †P<0.05 vs. ISO by one-way ANOVA with a Tukey posthoc test.

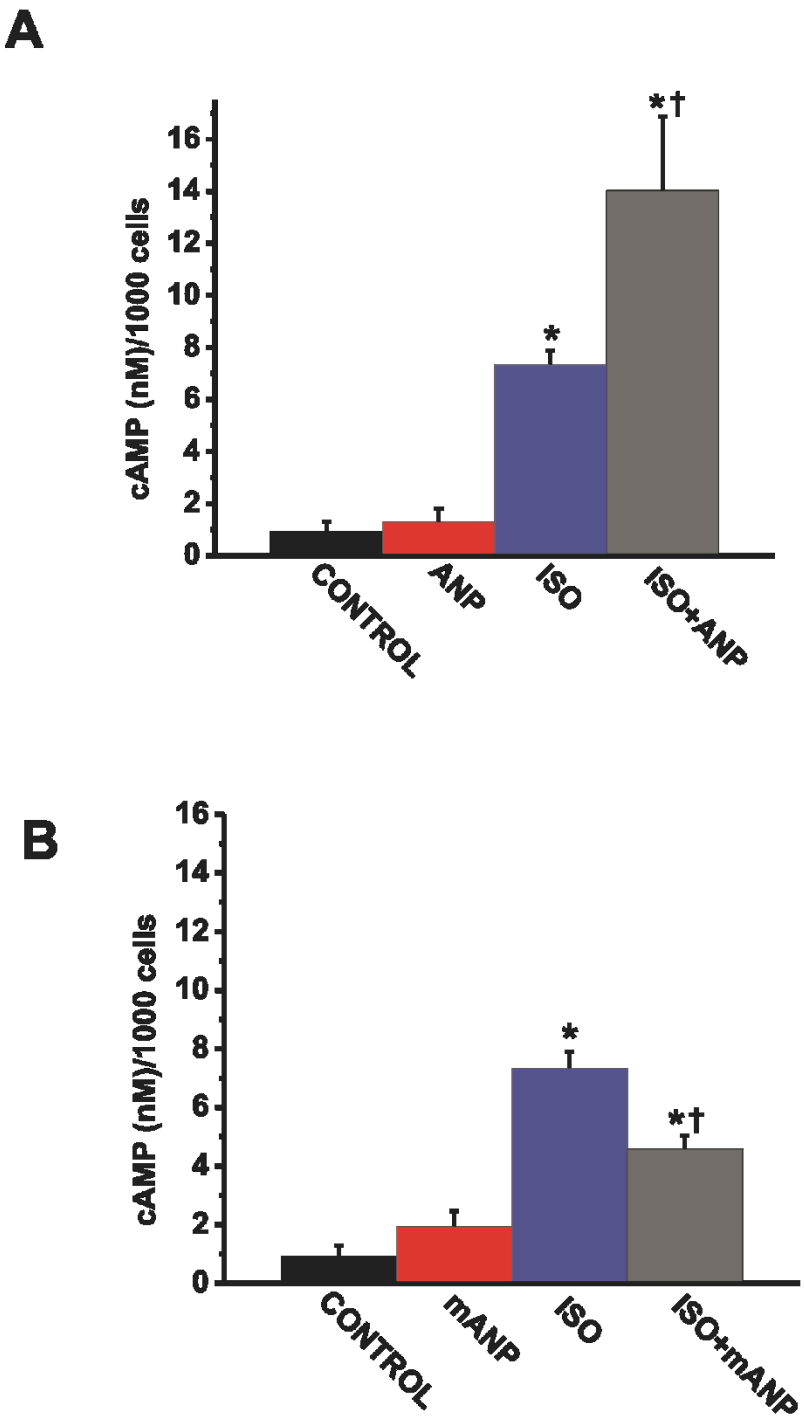
A
cAMP (nM)/1000 cells
0
2
4
6
8
10
12
14
16
*
*†
CONTROL
ANP
ISO
ISO+ANP
B
cAMP (nM)/1000 cells
0
2
4
6
8
10
12
14
16
*
*†
CONTROL
mANP
ISO
ISO+mANP

Figure 3.9

CHAPTER 4: DISCUSSION

4.1 Overview of Key Findings

ANP effects on atrial electrophysiology are unclear because a variety of species and techniques have been used in its study (Perrin & Gollob, 2012). The discovery of mANP and its association with AF (Hodgson-Zingman *et al*., 2008) has reinforced the importance of investigating the electrophysiological effects of NPs, including ANP, in the heart. Therefore, the purpose of this study was to investigate the electrophysiological effects of ANP and mANP and to determine which NPRs are involved in mediating their effects in mouse right atrial myocytes. We also investigated the intracellular signalling pathways that may be involved in mediating the effects of ANP and mANP.

The present study shows that ANP and mANP have opposing effects on $I_{Ca,L}$ and cAMP production in the presence of ISO in isolated mouse right atrial myocytes. In basal conditions, there were no observed effects of either ANP or mANP on atrial AP parameters or atrial $I_{Ca,L}$. However, in the presence of ISO (10 nM), ANP increased atrial $I_{Ca,L}$ and G_{max} while hyperpolarizing the $V_{1/2(act)}$. ANP's effects were maintained in right atrial myocytes isolated from NPR-$C^{-/-}$ mice and completely blocked when measured in the presence of the NPR-A antagonist A71915. In the presence of ISO, ANP also increased cAMP production in mouse right atrial myocytes. These observations show that ANP can increase atrial $I_{Ca,L}$ through NPR-A activation and that this occurs in association with an increase in cAMP concentrations in right atrial myocytes. The NPR-A dependent increase in $I_{Ca,L}$ elicited by ANP is likely due to a cGMP mediated inhibition of PDE3, which would result in increased cAMP levels (discussed further below).

The effects of mANP on atrial $I_{Ca,L}$ in the presence of ISO (10 nM) were markedly different from those seen with ANP. In the presence of ISO, mANP decreased atrial $I_{Ca,L}$ and G_{max} while depolarizing the $V_{1/2(act)}$. These effects were completely absent in right atrial myocytes isolated from NPR-$C^{-/-}$ mice. In the presence of ISO, mANP also decreased cAMP production in mouse right atrial myocytes. These observations show that mANP can decrease atrial $I_{Ca,L}$ through NPR-C activation in association with a decrease cAMP production. These unique mANP effects explain, at least partially, the mechanism by which mANP increases the occurrence of AF in affected patients.

4.2 Atrial Natriuretic Peptide Effects on Atrial Electrophysiology

It is known that ANP can activate NPR-A (Lucas *et al.,* 2000) and NPR-C (Bennett *et al*., 1991), and that these receptors modulate distinct downstream signalling pathways (Azer *et al*., 2012) (Fig 4.1). Previous work in our laboratory investigating the effects of BNP (which is highly related to ANP and also activates NPR-A and NPR-C) in mouse right atrial myocytes revealed a PDE3-dependent mechanism for increasing $I_{Ca,L}$ through NPR-A activation (Springer *et al*., 2012). Based on these results we hypothesized that ANP would act in a similar manner to BNP and increase atrial $I_{Ca,L}$ through NPR-A activation in the presence of ISO. The data presented in this study support this hypothesis. The effects of ANP on atrial $I_{Ca,L}$ were completely lost in the presence of the NPR-A antagonist A71915 (Delporte *et al*., 1992). Furthermore, we showed that the effects of ANP were not mediated through NPR-C as they were still present in NPR-$C^{-/-}$ mouse right atrial myocytes. These results clearly demonstrate that ANP activates and elicits its effects through NPR-A.

Figure 4.1: Potential mechanisms of ANP and mANP signalling. NPRA/B: natriuretic peptide receptors A and B; GC: guanylyl cyclase; cGMP: cyclic guanosine monophosphate; β-AR: β-adrenergic receptor; AC; adenylyl cyclacse; NPR-C: natriuretic peptide receptor C; G_i: inhibitory G-protein; αβγ: accessory G-protein subunits αβγ; cAMP: cyclic adenosine monophosphate; PDE3: phosphodiesterase 3; PDE2: phosphodiesterase 2; PKG: protein kinase G.

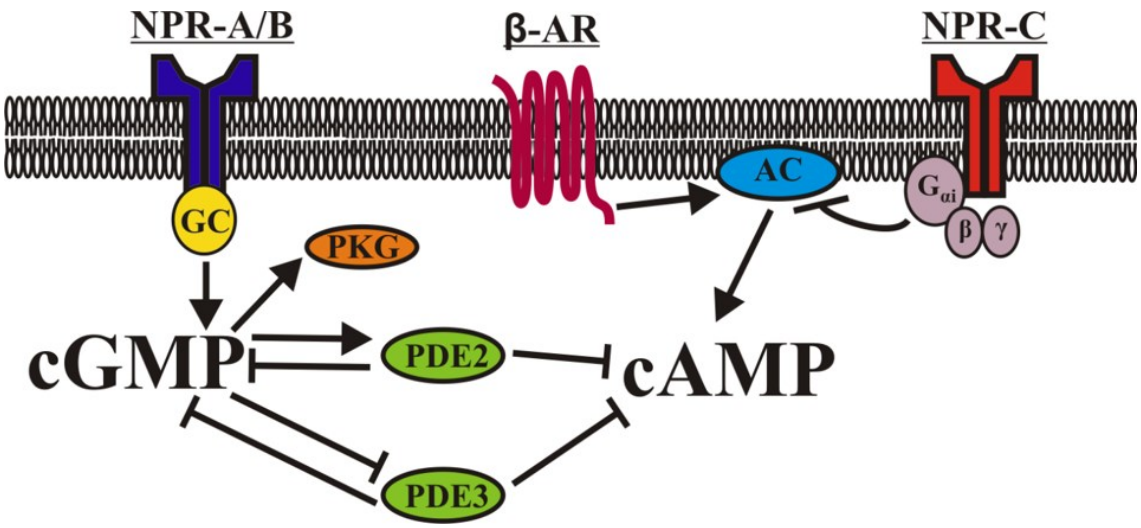

Figure 4.1

In basal conditions, ANP had no effect on atrial AP morphology or $I_{Ca,L}$. However, when pre-stimulated with the β-AR agonist ISO, ANP increased peak $I_{Ca,L}$ and cAMP production in mouse right atrial myocytes. We have previously shown that mouse atrial myocytes lack constitutive PDE3 activity in basal conditions (Hua *et al*., 2012; Springer *et al*., 2012), which explains why the NPR-A/PDE3 dependent effects of NPs (ANP and BNP) on atrial $I_{Ca,L}$ are only seen in the presence of ISO. β-ARs are linked to stimulatory G proteins (G_s) which, upon stimulation, increase AC activity. This leads to an increase in intracellular cAMP levels and stimulates phosphorylation of L-type calcium channels by PKA increasing channel activity (Xiao & Lakatta, 1993). PDE3, which hydrolyzes cAMP, is inhibited by cGMP (Omori & Kotera *et al*., 2007; Zaccolo & Movesian *et al*., 2007). Activation of NPR-A by its substrate ANP increases GC activity and cGMP concentrations (Chinkers *et al*., 1989; Schultz *et al.,* 1989). This increase in cGMP would inhibit the breakdown of cAMP via PDE3 allowing cAMP to stimulate calcium channels and thus increase $I_{Ca,L}$ as observed is this study. As discussed earlier in chapter 1.6, cyclic nucleotides affect PDEs in a concentration-dependent manner (Vandecasteele *et al*., 2001). At lower concentrations cGMP may stimulate PKGI activity which inhibits $I_{Ca,L}$. However with a larger concentration of cAMP the PKGI effect is displaced and the cAMP concentration is further elevated in a feed-forward mechanism due to the inhibition of PDE3. As a result $I_{Ca,L}$ is increased (Ono *et* al., 1991). This is consistent with our observations that ANP increased atrial $I_{Ca\,L}$ and cAMP production in the presence of ISO. With the increased pool of cAMP via ISO/β-AR/AC activity and increased pool of cGMP via ANP/NPR-A/GC, PDE3 hydrolysis of cAMP is inhibited and cAMP increases atrial $I_{Ca,L}$ through its effects on calcium channels. This result was reinforced using the

cAMP assay to measure cAMP levels upon ISO and ANP application. Application of ISO alone caused an increase in cAMP levels as is expected by its ability to increase AC activity. Application of ISO+ANP led to a further increase in cAMP, which can be explained by the cGMP-mediated inhibition of PDE3.

4.3 Mutant Atrial Natriuretic Peptide Effects on Atrial Electrophysiology

The presence of circulating mANP, produced by a mutation in the gene encoding ANP, predisposes patients to AF (Hodgson-Zingman *et al*., 2008). Similar to ANP, mANP has been shown to bind NPR-A and NPR-C (Dickey *et al*., 2009); however, the electrophysiological effects of mANP were largely unknown. We hypothesized that mANP would have unique electrophysiological effects through NPR signalling mechanisms that would lead to an increase in AF susceptibility. The data in this study supports the hypothesis. We showed that mANP effects on atrial $I_{Ca,L}$ were completely absent in NPR-$C^{-/-}$ mouse right atrial myocytes. This result clearly demonstrates that mANP activates and elicits its effects through NPR-C, in contrast to ANP's effects mediated through NPR-A.

Like ANP, mANP had no effects on atrial AP or atrial $I_{Ca\,L}$ in basal conditions. However, when pre-stimulated with the β-AR agonist ISO, mANP decreased peak $I_{Ca,L}$ and cAMP production in mouse right atrial myocytes. NPR-C is coupled to an inhibitory G protein (G_i) (Anand-Srivastava *et al*., 1996). G_i proteins directly inhibit AC activity and thus decrease cAMP levels (Anand-Srivastava *et al*., 1993; Rosa *et al*., 2003; Rose *et al*., 2004). Therefore, NPR-C stimulation by mANP would lead to a decrease in cAMP which would decrease PKA activity and thus inhibit calcium channel activation and $I_{Ca,L}$.

In basal conditions the activity of the AC may be too low for NPR-C/G_i activity to show its inhibitory effect. Consistent with this, we have previously shown that NPR-C mediated effects of NPs on ion channels in the heart are primarily seen in the presence of acute β-AR activation with ISO (Azer *et al*., 2012; Rose *et al*., 2003; Springer *et al*., 2012). In the case of mANP, the production of cAMP through β-AR activation would be directly affected by NPR-C rather than through a downstream PDE-dependent mechanism as proposed in ANP/NPR-A/GC signalling (Fig. 4.1). This result was reinforced using the cAMP assay to measure cAMP levels upon ISO and mANP application. Application of ISO alone caused an increase in cAMP levels as expected. Application of mANP in the presence of ISO led to a subsequent decrease in cAMP, which is consistent with the ability of NPR-C to inhibit AC activity following activation of G_i.

4.3.1 Mutant Atrial Natriuretic Peptide & Atrial Fibrillation

There are several mechanisms that initiate and/or sustain AF, including focal ectopic activity, re-entrant wave activity and slowed conduction (Nattel *et al*., 2008). Preliminary data from Hodgson-Zingman *et al*. showed a significant decrease in monophasic APD following application of mANP in a rat isolated heart model compared to WT ANP (Hodgson-Zingman *et al*., 2008). The data presented in this study are consistent with this finding as atrial $I_{Ca,L}$, an important determinant of APD, was significantly decreased in mouse right atrial myocytes upon mANP application. Shortening of the APD is predicted to favor electrical re-entry by decreasing the electrical wavelength. The wavelength is the distance that the electrical activity travels in one refractory period and is the product of

the refractory period and the conduction velocity (Nattel, 2002). The 'wavelength of re-entry', as described by Allessie *et al*., is the shortest path length that can sustain re-entrant electrical activity in the atria. For example, if the path length of the circuit is larger than the wavelength, the electrical activity will travel the circuit and return to its start point after the refractory period has ended. This results in a wave of electrical activity that is able to 're-enter' a circuit and propagate an electrical impulse in a series of re-entrant waves (Allessie *et al*., 1977; Nattel, 2002). Re-entry occurs when triggered ectopic activity is able to be propagated and sustained in a circuit through the atrial tissue (Skanes *et al*., 1998; Mandapati *et al*., 2000; Jalife *et al*., 2002). Focal ectopic activity is defined as automatic depolarization occurring in a region of the heart other than the SAN, i.e. the atria (Wit & Boyde, 2007).

The APD and effective refractory period (ERP) are important determinants of re-entry. Under normal conditions, re-entry does not occur because the conduction time of the wave is shorter than the ERP of the tissue and therefore it is unable to elicit inappropriate depolarizations that would be required to propagate a re-entrant wave. However, in situations where the ERP is shortened (or conduction is slowed) re-entry is more likely to occur. Shortened ERP is normally caused by a shortened APD. In this case the conduction time of the wave is longer than the ERP and the atrial tissue is able to be reactivated by the wave and propagate the activity through a circuit (Krogh-Madsen *et al*., 2012; Wakili *et al*., 2011). The effects of mANP on APD (Hodgson-Zingman *et al*., 2008) appear to be due to effects on atrial $I_{Ca,L}$ mediated through NPR-C/G_i effects on cAMP levels. The decrease in $I_{Ca,L}$ would decrease the length of the plateau phase of the AP, effectively shortening the APD and thus the ERP. The shortened ERP could enable

electrical wave propagation in the atria. While abbreviated refractoriness appears to be a link between mANP and increased AF susceptibility, further study is necessary to directly show mANP application leading to arrhythmia (this will be further discussed below in chapter 4.5).

While mANP was found to circulate at much higher concentrations than WT ANP (Hodgson-Zingman *et al*., 2008) due to a unique degradation profile (Dickey *et al*., 2009), Hodgson-Zingman *et al*.'s preliminary data and our study used WT ANP and mANP at the same concentration. Therefore the opposing effects of ANP and mANP are not due to a concentration-dependent mechanism. The implications of differing circulating concentration of mANP versus ANP are presently unclear.

Previous biochemical work showed that ANP and mANP are able to bind both NPR-A and NPR-C. Despite this, our experiments suggest that ANP and mANP affect atrial $I_{Ca,L}$ by signalling primarily through different NPRs; NPR-A and NPR-C, respectively. It is unknown why ANP does not appear to have NPR-C-dependent effects and why mANP does not appear to have NPR-A dependent effects in our experimental conditions. Binding assays for NPR-A and NPR-C, and activation assays for NPR-A, by ANP and mANP were done in human 293 cells expressing human NPR-A (Dickey *et al*., 2009). Schoenfeld *et al*. demonstrated marked differences in the ED_{50} and maximal cGMP responses between human, rat and mouse NPR-A (Shoenfeld *et al*., 1994). Also the majority of NPR binding and activation studies have been done in heterologous expression systems or kidney membrane preparations. This raises the question of species-dependent and tissue-dependent differences in NPR binding affinity and activation. To my knowledge no NPR binding or activation assays in cardiomyocytes have been done.

Other genetic variants in the gene encoding ANP have been associated with a cardiovascular disease phenotype. A population-based association study and follow-up mutational analysis in the Chinese population determined that the minor allele of single-nucleotide polymorphism (SNP) rs5063 in the *nppa* gene was associated with a significant risk of lone AF in Chinese patients (Ren *et al.*, 2010). However, this result could not be reproduced in two North American populations, including patients recruited at the Arrhythmia Clinic at the University of Ottawa Heart Institute (Roberts *et al*., 2010). In addition, a novel missense mutation was discovered in AF patients at nucleotide site 190 of the *nppa* gene. The location confers a mutation in the proANP peptide, which after further post-translational modification is not reflected in ANP but is within the vessel dilator peptide. This variant ANP produced a gain-of-function phenotype on the slow delayed rectifier potassium current, I_{Ks}, which was completely blocked with anantin application (Abraham *et al*., 2009). Anantin is an NPR-A antagonist (Weber *et al*., 1991). Computational simulations including the changes in I_{Ks} on a human atrial AP model resulted in a 37% shortening in atrial APD. This model also showed a loss of phase 2 of the AP which is largely due to $I_{Ca,L}$, indicating an impact of the variant ANP on atrial calcium current as well (Abraham *et al*., 2010). The reduction in $I_{Ca,L}$ and APD observed in this study could add further evidence to the theory of a reduced APD (and as a consequence ERP) as a substrate for re-entrant AF. Alterations in the ANP gene support its importance in atrial electrophysiology and how its modification can lead to arrhythmia.

4.4 Study limitations

The present study investigated the electrophysiological effects of ANP and mANP as well as their receptors in isolated mouse right atrial myocytes. This study only investigated the effects of ANP and mANP on mouse right atrial $I_{Ca,L.}$ There are other ion channels that exist in mouse atrial myocytes that may be regulated by these peptides that may underlie the NP signalling mechanisms, such as I_{Na} (Kecskemeti *et al.*, 1996; Sorbera & Morad, 1990), I_K and the ATP-sensitive potassium current I_{KATP} (Kecskemeti *et al.*, 1996). Also this study used only mouse atrial myocytes. The expression of PDEs and other important intracellular signalling molecules are species-dependent (Lugnier, 2006) and as previously discussed (see chapter 1.2) important ion channels (such as I_{Ks} and I_{Kr}) found in human atrial myocytes are absent in the mouse atria (Nerbonne, 2004). Future experiments could address these issues by investigating the effects of ANP and mANP on other ionic currents in atrial myocytes obtained from other species and /or humans. It is important to study the effects of ANP and mANP in human atrial myocytes as human myocytes have shown NP effects in basal conditions revealing that, in contrast to the mouse, human myocytes may have constitutive PDE3 activity (Le Grand *et al*., 1992).

It is also important to note that the patch clamp measurements were not done at the physiological temperature of 37°C. Temperature-dependant differences between room temperature and physiological temperature could be avoided by measuring currents at 37°C.

4.5 Future Directions

The purpose of this study was to investigate the electrophysiological effects of ANP and mANP in mouse right atrial myocytes. The results show that ANP activates NPR-A and through this mechanism can increase atrial $I_{Ca,L}$ and cAMP production. Previous work in our laboratory (Springer *et al*., 2008) has shown that BNP increases $I_{Ca,L}$ via NPR-A in a PDE3-dependent manner. While it is inferred that ANP also elicits its effects in a PDE3-dependent manner, experiments measuring $I_{Ca,L}$ in the presence of ISO and ANP should be repeated with the addition of the PDE3 inhibitor milrinone to conclusively show its role in ANP signalling.

There are multiple potential targets downstream from NPR-A activation. In addition to PDE3 regulation, cGMP activates PDE2. ANP's effects in the presence of a PDE2 inhibitor such as EHNA (Mery *et al*., 1995) may also prove to be an interesting signalling pathway. PDE2 hydrolyzes cAMP in the presence of cGMP and therefore when cGMP levels are elevated there is increased activation of PDE2 and increased hydrolysis of cAMP (Lugnier, 2006). As shown in previous work in our laboratory mouse atrial $I_{Ca,L}$ was increased upon EHNA application (Hua *et al*., 2013). With the application of ISO and ANP an even further increase in $I_{Ca,L}$ would be expected upon EHNA application because of a higher level of intracellular cAMP. This would add to the important role of PDEs in mediating NPs effects on cardiac electrophysiology.

In addition to PDE2, cGMP can also increase PKG activity. PKGI is thought to inhibit $I_{Ca,L}$ indirectly, by increasing potassium currents and hyperpolarizing the membrane (Alioua *et al*., 1998; Swayze *et al*., 2001), and directly through phosphorylation of the channel or associated regulatory proteins (Potter *et al*., 2006). The effects of PKGI

activity through NPR-A activation could also be an interesting area of study, especially with its inhibitory effects on $I_{Ca,L}$ which may lead to APD shortening and an increase in AF susceptibility.

In terms of mANP and its relationship to AF, using high resolution optical mapping and *in vivo* administration of the mutant peptide could provide further mechanistic information and evidence that mANP does in fact lead to an increase in AF predisposition. Optical mapping can measure conduction speed (an important determinant of AF susceptibility (Nattel *et al*., 2008)) across an atrial preparation and with stimulation may show re-entrant electrical waves, or rotors, upon mANP application - if this is indeed how mANP elicits its effects. Following application of mANP AF inducibility *in vivo* could be measured during burst pacing in the atria (Fukui *et al*., 2003).

4.6 Conclusions

In summary, the present study shows that ANP and mANP have no effect on basal AP morphology or $I_{Ca,L}$ in mouse right atrial myocytes. This may be due to lack of constitutive PDE activity and low AC activity in atrial myocytes. In the presence of ISO, ANP increases atrial $I_{Ca,L}$ and cAMP production via NPR-A activation. The mechanism is presumed to be dependent on PDE3 activity as shown by previous work in our laboratory (Springer *et al*., 2012). In contrast, in the presence of ISO, mANP primarily elicits its effects through NPR-C and decreases atrial $I_{Ca,L}$ and cAMP production. This observation supports a critical signalling role for NPR-C in the atria. The inhibitory effect of mANP on atrial $I_{Ca,L}$ also reveals a possible mechanism by which mANP may shorten

monophasic APD (Hodgson-Zingman *et al*., 2008) and produce a substrate for re-entrant electrical activity and AF (Nattel *et al*., 2008).

Based on these and previous findings it is clear that NPs play an important regulatory role in atrial electrophysiology. The mechanisms by which NPs elicit their responses are complex and involve multiple NPRs and downstream signalling pathways. Pathology associated with mutations in NPs or their receptors also support their vital physiological role. The results presented in this thesis provide novel insight into NP effects on atrial electrophysiology and reveal a unique mechanism by which mutations in the NP system may lead to arrhythmogenesis. This research improves our understanding of NPs effects in both physiological and pathophysiological conditions, such as AF.

REFERENCES

Abraham R, Yang T, Blair M, Roden D, Darbar D. (2010). Augmented potassium current is a shared phenotype for two genetic defects associated with familial atrial fibrillation. *J Mol Cell Cardiol*. **48:** 181-190.

Alioua A, Tanaka Y, Wallner M, Hofmann F, Ruth P, Meera P, Toro L. (1998). The large conductance, voltage-dependent, and calcium-sensitive K channel, Hslo, is a target of cGMP-dependent protein kinase phosphorylation in vivo. *J Biol Chem*. **273:**32950–32956.

Allessie M, Bonke F, Schopman F. (1977). Circus movement in rabbit atrial muscle as a mechanism of tachycardia. III. The "leading circle" concept: a new model of a circus movement in cardiac tissue without the involvement of an anatomical obstacle. *Circ Res.* **41:** 9-18.

Altier C, Garcia-Caballero A, Simms B, You H, Chen L, Walcher J, Tedford H, Hermosilla T,Zamponi G. (2011). The $Ca_v\beta$ subunit prevents RFP2-mediated ubiquitination and proteasomal degradation of L-type channels. *Nat Neurosci.* **14:**173–180.

Anand-Srivastava M, Genest J, Cantin M. (1985). Inhibitory effect of atrial natriuretic factor onadenylate cyclase activity in adrenal cortical membranes. *FEBS Lett.* **181:** 199-202.

Anand-Srivastava MB, Cantin M. (1986). Atrial natriuretic factor receptors are negatively coupled to adenylate cyclase in cultured atrial and ventricular cardiomyocytes. *Biochem Biophys Res Commun.* **138:** 427-436.

Anand-Srivastava M, Srivastava A, Cantin M. (1987). Pertussis toxin attenuates atrial natriuretic factor-mediated inhibition of adenylate cyclase. Involvement of inhibitory guanine nucleotide regulatory protein. *J Biol Chem.* **262:** 4931-4934.

Anand-Srivastava M, Gutkowska J, Cantin M. (1991). The presence of atrial-natriuretic factor receptors of ANF-R2 subtype in rat platelets. Coupling to adenylate cyclase/cyclic AMP signal-transduction system. *Biochemical Journal.* **278:** 211-217.

Anand-Srivastava M & Trachte G. (1993). Atrial natriuretic factor receptors and signal transduction mechanisms. *Pharmacological reviews.* **45:** 455-497.

Anand-Srivastava M, Sehl P, Lowe D. (1996). Cytoplasmic domain of natriuretic peptide receptor-C inhibits adenylyl cyclase. Involvement of a pertussis toxin-sensitive G protein.m*J Biol Chem.* **271:** 19324-19329.

Anand-Srivastava M. (2005). Natriuretic peptide receptor-C signalling and regulation. *Peptides.***26:** 1044-1059.

Antzelevitch C, Pollevick G, Cordeiro JM, Casis O, Sanguinetti M, Aizawa Y, Guerchicoff A,Pfeiffer R, Olivia A, Wollnik B, Gelber P, Bonaros E, Burashnikov E, Wu Y, Sargent J, Schickel S, Oberheiden R, Bhatia A, Hsu L, Haissaguerre M, Schimpf R, Borggree M, Wolpert C. (2007). Loss-of-function mutations in the cardiac calcium channel underlie a new clinical entity characterized by ST-segment elevation, short QT intervals, and sudden cardiac death. *Circulation.* **115:**442–449.

Azer J, Hua R, Vella K, Rose R. (2012). Natriuretic peptides regulate heart rate and sinoatrial node function by activating multiple peptide receptors. *J Mol Cell Cardiol.* **53:** 715-724.

Bangalore R, Mehrke G, Gingrich K, Hofmann F, Kass R. (1996). Influence of L-type Ca channel α_2/γ-subunit on ionic and gating current in transiently transfected HEK 293 cells.*Am J Physiol.* **270:**1521-1528.

Barbee R, Perry B, Re R, Murgo J, Field L. (1994). Hemodynamics in transgenic mice with overexpression of atrial natriuretic factor. *Circ Res.***74:**747–751.

Bauer C, Tran-Van-Minh A, Kadurin I, Dolphin A. (2010). A new look at calcium channel $\alpha_2\gamma$ subunits. *Curr Opin Neurobiol.* **20:**563–571.

Baxter G. (2004). The natriuretic peptides: An introduction. *Basic Res Cardiol.* **99:**71-75.

Beavo J. (1995). Cyclic nucleotide phosphodiesterases: functional implications of multipleisoforms. *Physiol Rev.* **75:**725-748.

Bender A & Beavo J (2006). Cyclic nucleotide phosphodiesterases: molecular regulation to clinical use. *Pharmacol Rev.* **58:** 488-520.

Benjamin E, Levy D, Vaziri S, D'Agostino R, Belanger A, Wolf P. (1994). Independent risk factors for atrial fibrillation in a population-based cohort: the Framingham Heart Study. *The Journal of the American Medical Association.* **271:**840-844.

Benjamin E, Wolf P, D-Agostino R, Silbershatz H, Kanel W, Levy D. (1998). Impact of atrial fibrillation on the risk of death the Framingham Heart Study. *Circulation*. **98:** 946-952.

Benjamin E, Chen P, Bild D, Mascette A, Albert C, Alnso A, Calkins H, Connolly S, Curtis A, Darbar D, Ellinor P, Go A, Goldschlager N, Heckbert S, Jalife J, Kerr C, Levy D, Lloyd-Jones D, Massie B, Nattel S, Olgin J, Packer D, Po S, Tsang T, Van Wagoner D, Waldo A, Wyse D. (2009). Prevention of atrial fibrillation: report from a national lung, heart and blood institute workshop. *Circulation*. **119:** 606-618

Bennett B, Bennett G, Vitangcol R, Jewett J, Burnier J, Henzel W, Lowe D. (1991). Extracellular domain-IgG fusion proteins for three human natriuretic peptide

receptors. Hormone pharmacology and application to solid phase screening of synthetic peptide antisera. *J Biol Chem.* **266:** 23060-23067.

Bianchi C, Anand-Srivastava M, De Léan A, Gutkowska J, Forthomme D, Genest J, Cantin M. (1986). Localization and characterization of specific receptors for atrial natriuretic factor in the ciliary processes of the eye. *Curr Eye Res.* **5:** 283-293.

Bkaily G, Perron N, Wang S, Sculptoreanu A, Jacques D, Menard D. (1993). Atrial natriuretic factor blocks the high threshold Ca^{2+} current and increases K^{+} current in fetal single ventricular cells. *JMCC*. **11:** 1305-1316.

Buraei Z & Yang J. (2010). The βsubunit of voltage-gated Ca^{2+} channels. *Physiol Rev.* **90:**1461–1506.

Cao L & Gardner D. (1995). Natriuretic peptides inhibit DNA synthesis in cardiac fibroblasts. *Hypertension.* **25:**227–234.

Carvajal J, Germain A, Huidobro-Toro J, Weiner C. (2000). Molecular mechanism of cGMP-mediated smooth muscle relaxation. *J Cell Physiol.* **184:**409–420.

Catterall W. (2000). Structure and regulation of voltage-gated Ca2+ channels. *Annu Rev Cell Dev Biol.* **16:** 521–555.

Chen Y, Li M, Zhang Y, He L, Yamada Y, Fitzmaurice A, Shen Y, Zhang H, Tong L, Yang J. (2004). Structural basis of the α_1-β subunit interaction of voltage-gated Ca^{2+} channels. *Nature.* **429:**675–680.

Chinkers M, Garbers D, Chang M, Lowe D, Chin H, Goeddel D, Schulz S. (1989). A membrane form of guanylate cyclase is an atrial natriuretic peptide receptor. *Nature London.* **338:** 78-83.

Chu P, Robertson H, Best P. (2001). Calcium channel gamma subunits provide insights into the evolution of this gene family. *Gene.* **280:**37–48.

Cody R, Atlas S, Laragh J, Kubo S, Covit A, Ryman K, Shaknovich A, Pondolfino K, Clark M, Camargo M. (1986). Atrial natriuretic factor in normal subjects and heart failure patients. Plasma levels and renal, hormonal, and hemodynamic responses to peptide infusion. *Journal of Clinical Investigation.* **78:** 1362 1374.

Collin T, Wang J, Nargeot J, Schwartz A. (1993). Molecular cloning of three isoforms of the L-type voltage-dependent calcum channel β subunit from normal human heart. *Circulation Research*. **72:** 1337-1344.

Conti M & Beavo J. (2007). Biochemistry and physiology of cyclic nucleotide phosphodiesterases: essential components in cyclic nucleotide signalling. *Annu Rev Biochem.* **76:** 481-511.

Dai S, Hall D, Hell J. (2009). Supramolecular assemblies and localized regulation of voltage-gated ion channels. *Physiol Rev*. **89:**411–452.

de Bold A, Borenstein H, Veress A, Sonnenberg H. (1981). A rapid and potent natriuretic response to intravenous injection of atrial myocardial extract in rats. *Life Sci*. **28:** 89-94.

de Léan A, Gutkowska J, McNicoll N, Schiller PW, Cantin M, Genest J. (1984). Characterization of specific receptors for atrial natriuretic factor in bovine adrenal zona glomerulosa. *Life Sci.* **35:** 2311-2318.

Delporte C, Winand J, Poloczek P, Von Geldern T, Christophe J. (1992). Discovery of a potent atrial natriuretic peptide antagonist for ANPA receptors in the human neuroblastoma NB-OK-1 cell line. *Eur J Pharmacol.* **224:** 183-188.

Dickey D, Yoder A, Potter L. (2009). A familial mutation renders atrial natriuretic peptide resistant to proteolytic degradation. *J Biol Chem.* **284:** 19196-19202.

Dobrev D & Nattel S. (2010). New antiarrhythmic drugs for treatment of atrial fibrillation. *Lancet*. **375:**1212–1223.

Dolphin A. (2003). Beta subunits of voltage-gated calcium channels. *J Bioenerg Biom Embr.***35:**599–620.

Dolphin A. (2012). Calcium channel auxiliary $\alpha_2\gamma$ and β subunits: trafficking and one step beyond. *Nat Rev Neurosci.* **13:**542–555.

Doyle D, Ambler S, Upshaw-Earley J, Bastawrous A, Goings G, Page E. (1997). Type B atrial natriuretic peptide preceptor in cardiac myocytes caveolae. *Circ Res.* **81:** 86–91.

D'Souza S, Davis M, Baxter G. (2004). Autocrine and paracrine actions of natriuretic peptides in the heart. *Pharmacol Ther.* **101:** 113-129.

Edwards B, Zimmerman R, Schwab T, Heublein D, Burnett J. (1988). Atrial stretch, not pressure, is the principal determinant controlling the acute release of atrial natriuretic factor. *Circ Res.* **62:** 191-195.

Erdos E & Skidgel R. (1989). Neutral endopeptidase 24.11 (enkephalinase) and related regulators of peptide hormones. *The FASEB journal.* **3:** 145-151.

Erickson M, Alseikhan B, Peterson B, Yue D. (2001). Preassociation of calmodulin with voltage-gated Ca^{2+} channels revealed by FRET in single living cells. *Neuron.* **31:**973–985.

Fan D, Bryan P, Ants L, Potthast R, Potter L. (2004). Downreglation does not mediate natriuretic peptide-dependent desensitization of natriuretic peptide receptor (NPR)-A

or NPR-B: guanylyl cyclase-linked natriuretic peptide receptors do not internalize. *Mol Pharmacol*. **67:** 174-183.

Fang K & Colecraft H. (2011).Mechanism of auxiliary beta-subunit-mediated membrane targeting of L-type ($Ca_V1.2$) channels. *J Physiol*. **589:**4437–4455.

Féthière J, Graihle R, De Léan A. (1992). Identification of the atrial natriuretic factor-R1C receptor subtype (B-clone) in cultured rat aortic smooth muscle cells. *FEBS Lett.* **305:**77-80.

Fischmeister R, Castro L, Abi-Gerges A, Rochais F, Jurevicius J, Leroy J, Vandecasteele G. (2006). Compartmentation of cyclic nucleotide signalling in the heart: the role of cyclic nucleotide phosphodiesterases. *Circ Res.* **99:** 816-828.

Foster D & Garbers D. (1998). Dual role for adenine nucleotides in the regulation of the atrial natriuretic peptide receptor, guanylyl cyclase-A. *J Biol Chem.* **273:** 16311-16318.

Francis S, Turko I, Corbin J. (2001). Cyclic nucleotide phosphodiesterases: relating structure and function. *Prog Nucleic Acid Res Mol Biol* **65:** 1-52.

Francis S, Blount M, Corbin J. (2011). Mammalian cyclic nucleotide phosphodiesterases: molecular mechanisms and physiological functions. *Physiol Rev.* **91:** 651-690.

Franco F, Dubois S, Peshock R, Shohet R. (1998). Magnetic resonance imaging accurately estimates LV mass in a transgenic mouse model of cardiac hypertrophy. *Am J Physiol.***274:** 679-683.

Foell J, Balijepalli R, Delisle B, Yunker A, Robia S, Walker J, McEnery M, January C, Kamp T. (2004). Molecular heterogeneity of calcium channel beta-subunits in canine and human heart: evidence for differential subcellular localization. *Physiol Genomics*. **17:**183–200.

Fukui A, Takahasi N, Nakada C, Masaki T, Kume O, Shinohara T, Teshima Y, Hara M, Saikawa T. (2013). Role of leptin signalling in the pathogenesis of angiotensin II-mediated atrial fibrosis and fibrillation. *Circ Arrhythm Electrophysiol*. **6:**402-409.

Fuller-Bicer G, Varadi G, Koch S, Ishii M, Bodi I, Kadeer N, Muth J, Mikala, G, Petrashevskaya N, Jordan M, Zhang S, Qin N, Flores C, Isaacsohn, I, Varadi M, Mori Y, Jones W, Schwartz A. (2009). Targeted disruption of the voltage-dependent calcium channel α_2/γ_1-subunit. *Am J Physiol Heart Circ Physiol.* **297:**117-124.

Fuster V, Ryden L, Cannom D, Crijins H, Curtis A, Ellenbogen K, Halperin J, Kay G, Le Huezey J, Lowe J, Olsson S, Prystowsky E, Tamargo J, Wann L. (2011). 2011 ACCF/AHA/HRS focused updates incorporated into the ACC/AHA/ESC 2006 guidelines for the management of patients with atrial fibrillation: a report of the

American College of Cardiology Foundation/American Heart Association Task Force on Practice Guidelines developed in partnership with the European Society of Cardiology and in collaboration with the European Heart Rhythm Association and the Heart Rhythm Society. *J Am Coll Cardiol*. **57:** 101-198.

Gao B, Sekido Y, Maximov A, Saad M, Forgacs E, Latif F, Wei M, Lee J, Perez-Reyes E, Bezprozvanny I, Minna J. (2000). Functional properties of a new voltage-dependent calcium channel $\alpha_2\gamma$auxiliary subunit gene (CACNA2D2). *J Biol Chem.* **275:**12237–12242.

Gisbert M & Fischmeister R. (1988). Atrial natriuretic factor regulates the calcium current in frog isolated cardiac cells. *Circ Res*. **62:** 660-667.

Halling D, Aracena-Parks P, Hamilton S. (2005). Regulation of voltage-gated Ca^{2+} channels bycalmodulin. *Sci STKE*. **2005:** re15.

Hamill O, Marty A, Neher E, Sakmann B, Sigworth F. (1981). Improved patch-clamp techniques for high-resolution current recording from cells and cell-free membrane patches. *Pflugers Arch.* **391:** 85-100.

Hatano S, Yamashita T, Sekiguchi A, Iwasaki Y, Nakazawa K, Sagara K, Iinuma H, Aizawa T, Fu L. (2006). Molecular and electrophysiological differences in the L-type Ca^{2+} channel of the atrium and ventricle of rat hearts. *Circ J*. **70:** 610-614.

Heart and Stroke Foundation. Statistics. 2013. Received from http://www.heartandstroke.com/site/c.ikIQLcMWJtE/b.3483991/k.34A8/Statistics.htm#references.

Hodgson-Zingman D, Karst M, Zingman L, Heublein D, Darbar D, Herron K, Ballew J, de Andrade M, Burnett Jr J, Olson T. (2000). Atrial natriuretic peptide frameshift mutation in familial atrial fibrillation. *N Engl J Med.* **359:** 158-165.

Hofmann F, Ammendola A, Schlossmann J. (2000). Rising behind NO: cGMP-dependent protein kinases. *J Cell Sci.* **113:**1671–1676.

Holtwick R, Van Eickels M, Skryabin B, Baba HA, Bubikat A, Begrow F, Schneider M, Garbers D, Kuhn M. (2003). Pressure independent cardiac hypertrophy in mice with cardiomyocyte restricted inactivation of the atrial natriuretic peptide receptor guanylyl cyclase-A. *J Clin Invest.* **111:**1399–1407.

Hua R, Adamczyk A, Robbins C, Rosa R. (2012). Distinct Patterns of constitutive phosphodiesterase activity in mouse sinoatrial node and atrial myocardium. *PLoS One.* **7:** e47652.

Hunt P, Espiner E, Nicholls M, Richards A, Yandle T. (1996). Differing biological effects of equimolar atrial and brain natriuretic peptide infusions in normal man. *J Clin Endocrinol Metab.* **81:** 3871-3876.

Huxley V, Tucker V, Verburg K, Freeman R. (1987). Increased capillary hydraulic conductivity induced by atrial natriuretic peptide. *Circ Res*. **60:**304–307.

Inaba, H, Hayami, N, Ajiki, K, Sugishita, Y, Kunishima T, Yamagishi N, Yamagishi S, Murakawa Y. (2008) Human atrial natriuretic peptide suppresses Torsades de Pointe in rabbits. *Circulation.* **72:** 820-824.

Jalife J, Berenfeld O, Mansour M. (2002). Mother rotors and fibrillatory conduction: a mechanism of atrial fibrillation. *Cardiovasc Res*. **54:** 204-216.

Jaubert J, Jaubert F, Martin N, Washburn L, Lee B, Eicher E, Guénet J. (1999). Three new allelic mouse mutations that cause skeletal overgrowth involve the natriuretic peptide receptor C gene (Npr3). *Proc Natl Acad Sci USA.* **96:** 10278-10283.

Jewett J, Koller K, Goeddel D, Lowe D. (1993). Hormonal induction of low affinity receptor guanylyl cyclase. *EMBO J.* **12:** 769-777.

John S, Krege J, Oliver P, Hagaman J, Hodgin J, Pang S, Flyn T, Smithies O. (1995). Genetic decreases in atrial natriuretic peptide and salt-sensitive hypertension. *Science*. **267:** 679- 681.

John S, Veress A, Honrath U, Chong C, Peng L, Smithies O, Sonnenberg H. (1996). Blood pressure and fluid-electrolyte balance in mice with reduced or absent ANP. *American Journal of Physiology-Regulatory, Integrative and Comparative Physiology*. **271:** 109-114.

Johns D, Ao Z, Heidrich B, Hunsberger G, Graham T, Payne L, Elshourbagy, Lu Q, Aiyar N, Douglas S. (2007). Dendroaspis natriuretic peptide binds to the natriuretic peptide clearance receptor. *Biochemical and Biophysical Research Communications.* **358:**145-149.

Kapoun A, Liang F, O'Young G, Damm D, Quon D, White R, Munson K, Lam A, Schreiner G, Protter A. (2004). B-type natriuretic peptide exerts broad functional opposition to transforming growth factor-_ in primary human cardiac fibroblasts: fibrosis, myofibroblast conversion, proliferation, and inflammation. *Circ Res.* **94:**453–461.

Katz A. (2010). *Physiology of the Heart (5 Ed.)*. Lippincott Williams & Wilkins, Philadelphia, PA.

Kaupp U & Seifert R. (2002). Cyclic nucleotide-gated ion channels. *Physiol Rev.* **82:**769–824.

Kecskemeti V, Pacher P, Pankucsi C, Nanasi P. (1996). Comparative study of cardiac electrophysiological effects of atrial natriuretic peptide. *Mol Cell Biochem*. **160/161:** 53-59.

Kenny A, Bourne A, Ingram J. (1993). Hydrolysis of human and pig brain natriuretic peptides, urodilatin, C-type natriuretic peptide and some C-receptor ligands by endopeptidase-24.11. *Biochem J.* **291:** 83-88.

Kim S, Kim Y, Kim S, Kim S, Cho K, Kim S. (2011). Presence of *Dendroaspis* natriuretic peptide and its binding to NPR-A receptor in rabbit kidney. *Regulatory Peptides.* **167:**42-49.

Kishimoto I, Rossi K, Garbers D. (2001). A genetic model provides evidence that the receptor for atrial natriuretic peptide (guanylyl cyclase-A) inhibits cardiac ventricular myocyte hypertrophy. *Proc Natl Acad Sci USA*. **98:** 2703-2706.

Knowles J, Esposito G, Mao L, Hagaman J, Fox J, Smithies O, Rockman H, Maeda N. (2001). Pressure-independent enhancement of cardiac hypertrophy in natriuretic peptide receptor A-deficient mice. *J Clin Invest.* **107:**975–984.

Kojda G, Kottenberg K, Nix P, Schluter K, Piper H, Noack E. (1996). Low increase in cGMP induced organic nitrates and nitrovasodilators improves contractile response of rat ventricular myocytes. *Circ Res*. **78:** 91-101.

Koschak A, Reimer D, Huber I, Grabner M, Glossmann H, Engel J & Striessnig J. (2001). α_{1D} ($Ca_v1.3$) subunits can form L-type Ca^{2+} channels activating at negative voltages. *J Biol Chem.* **276:** 22100-22106.

Kostic M, Erdogan S, Rena G, Borchert G, Hoch B, Bartel S, Scotland G, Huston E, Houslay M,
Krause E. (1997). Altered expression of PDE1 and PDE4 cyclic nucleotide phosphodiesterase isoforms in 7-oxo-prostacyclin preconditioned rat heart. *J Mol Cell Cardiol.* **29:** 3135-3146.

Krogh-Madsen T, Abbott G, Christini D. (2012). Effects of electrical and structural remodelling on atrial fibrillation maintenance: a simulation study. *PLoS Comput Biol*. **8:** e1002390.

Kuhn M. (2004). Molecular physiology of natriuretic peptide signalling. *Basic Res Cardiol.* **99:** 76-82.

Lainchbury J, Meyer D, Jougasaki M, Burnett J, Redfield M. (2000). Effects of natriuretic peptides on load and myocardial function in normal and heart failure dogs. *Am J Physiol Heart Circ Physiol*. **278:** 33-40.

Le Grand B, Deroubaix E, Couétil J, Coraboeuf E. (1992). Effects of atrionatriuretic factor on Ca^{2+} current and Ca-independent transient outward K+ current in human atrial cells. *Pflugers Arch.* **421:** 486-491.

Levin E, Gardner D, Samson W. (1998). Natriuretic peptides. *N Engl J Med.* **339:** 321-328.

Levi R, Alloatti G, Fischmeister R. (1989). Cyclic GMP regulates the Ca-channel current in guinea pig ventricular myocytes. *Pflügers Archiv European Journal of Physiology.* **413:** 685-687.

Lopez M, Wong S, Kishimoto I, Dubois S, Mach V, Friesen J, Garbers D, Beuve A. (1995). Salt-resistant hypertension in mice lacking the guanylyl cyclase-A receptor for atrial natriuretic peptide. *Nature.* **378:** 65-68.

Lopez M, Garbers D, Kuhn M. (1997). The guanylyl cyclase-deficient mouse defines differential pathways of natriuretic peptide signalling. *J Biol Chem.* **272:** 23064-23068.

Loughney K, Martins T, Harris E, Sadhu K, Hicks J, Sonnenburg W, Beavo J, Ferguson K. (1996). Isolation and characterization of cDNAs corresponding to two human calcium, calmodulin-regulated, 3', 5'-cyclic nucleotide phosphodiesterases. *J Biol Chem.* **271:** 796-806.

Lowe D, Chang M, Hellmiss R, Chen E, Singh S, Garbers D, Goeddel D. (1989). Human atrial natriuretic peptide receptor defines a new paradigm for second messenger signal transduction. *EMBO J.* **8:** 1377-1384.

Lucas K, Pitari G, Kazerounian S, Ruiz-Stewart I, Park J, Schulz S, Chepenik K, Waldman S.(2000). Guanylyl cyclases and signalling by cyclic GMP. *Pharmacol Rev.* **52:** 375-414.

Lugnier C. (2006). Cyclic nucleotide phosphodiesterase (PDE) superfamily: a new target for the development of specific therapeutic agents. *Pharmacol Ther.* **109:** 366-398.

Maack T, Suzuki M, Almeida F, Nussenzveig D, Scarborough R, McEnroe G, Lewicki J. (1987). Physiological role of silent receptors of atrial natriuretic factor. *Science.* **238:** 675-678.

Mandipati, R, Skanes A, Chen J, Berefeld O, Jalife J. Stable microreentrant sources as a mechanism of atrial fibrillation in the isolated sheep heart. *Circulation.* **101:** 194-199.

Mangoni M, Couette B, Bourinet E, Platzer J, Reimer D, Striessnig J, Nargeot J. (2003). Functional role of L-type Cav1.3 Ca2+ channels in cardiac pacemaker activity. *PNAS.* **100:** 5543-5548.

Marin-Grez M, Fleming J, Steinhausen M. (1986). Atrial natriuretic peptide causes preglomerular vasodilatation and post-glomerular vasoconstriction in rat kidney. *Nature.* **324:** 473-476.

Matsukawa N, Grzesik W, Takahashi N, Pandey K, Pang S, Yamauchi M, Smithies O. (1999). The natriuretic peptide clearance receptor locally modulates the physiological effects of the natriuretic peptide system. *Proc Natl Acad Sci USA*. **96:**7403-7408.

Maurice D, Palmer D, Tilley D, Dunkerley H, Netherton S, Raymond D, Elbatarny H, Jimmo S. (2003). Cyclic nucleotide phosphodiesterase activity, expression, and targeting in cells of the cardiovascular system. *Mol Pharmacol*. **64:** 533-546.

McCall D & Fried T. (1990). Effect of atriopeptin II on Ca influx, contractile behavior and cyclic nucleotide content of cultured neonatal rat myocardial cell. *J Mol Cell Cardiol.* **22:**1-212.

McKay M & Huxley V. (1995). ANP increases capillary permeability to protein independent of perfusate protein composition. *Am J Physiol.* **268:**1139-1148.

Meacci E, aira M, Moos M, Smith C, Movesian M, Degerman E, Belfrage P, Manganiello V. (1992). Molecular cloning and expression of human myocardial cGMP-inhibited cAMP phosphodiesterases. *Proc Natl Acad Sci USA*. **89:** 3721-3725.

Méry P, Lohmann S, Walter U, Fischmeister R. (1991). Ca^{2+} current is regulated by cyclic GMP-dependent protein kinase in mammalian cardiac myocytes. *Proc Natl Acad Sci USA*. **88:** 1197-1201.

Méry P, Pavoine C, Pecker F, Fischmeister R. (1995). Erythro-9-(2-hydroxy-3-nonyl) adenine inhibits cyclic GMP-stimulated phosphodiesterase in isolated cardiac myocytes. *Mol Pharmacol.* **48:** 121-130.

Meissner M, Weissgerber P, Londono J, Prenen J, Lnk S, Ruppenthal S, Molkentin J, Lipp P, Nilius B, Freichel M, Flockerzi V. (2011). Moderate calcium channel dysfunction in adult mice with inducible cardiomyocytes-specific excision of the cacnb2 gene. *J Biol Chem.* **286:** 15875-15882.

Miao L, Yin M, Yuan W, Chen Q, Fleischmann Y, Hescheler B, Ji J, Guangju. (2010). Atrial Natriuretic Peptide Regulates Ca^{2+} Channel in Early Developmental Cardiomyocytes. *PLoS One.* **5:** e8847.

Misono K, Grammer R, Fukumi H, Inagami T. (1984). Rat atrial natriuretic factor: isolation, structure and biological activities of four major peptides. *Biochem Biophys Res Commun.* **123:** 444-451.

Movesian, M. (2002). PDE3 cyclic nucleotide phosphodiesterases and the compartmentation of cyclic nucleotide-mediated signalling in cardiac myocytes. *Basic Res Cardiol*. **97:** 183-190.

Nagase M, Katafuchi T, Hirose S, Fujita T. (1997). Tissue distribution and localization of natriuretic peptide receptor subtypes in stroke prone spontaneously hypertensive rats. *J Hypertens*. **15:**1235–1243.

Nattel S. (2002). New ideas about atrial fibrillation 50 years on. *Nat Rev*. **415:** 219-226.

Nattel S, Burstein B, Dobrev D. (2008). Atrial remodeling and atrial fibrillation. *Circulation:Arrhythmia and Electrophysiology.* **1:** 62-73.

Nerbonne JM. (2004). Studying cardiac arrhythmias in the mouse - a reasonable model for probing mechanisms? *Trends in Cardiovascular Medicine.* **14:** 83-93.

Nerbonne J & Kass R. (2005). Molecular physiology of cardiac repolarization. *Science's STKE.* **85:** 1205-1253.

Nussenzveig D, Lewicki J, Maack T. (1990). Cellular mechanisms of the clearance function of type C receptors of atrial natriuretic factor. *J Biol Chem.* **265:** 20952-20958.

Ogawa Y, Itoh H, Tamura N, Suga S, Yoshimasa T, Uehira M, Matsuda S, Shiono S, Nishimoto H, Nakao K. (1994). Molecular cloning of the complementary DNA and gene that encode mouse brain natriuretic peptide and generation of transgenic mice that overexpress the brain natriuretic peptide gene. *J Clin Invest.* **93:** 1911-1921.

Oliver P, Fox J, Kim R, Rockman H, Kim H, Reddick R, Pandey K, Milgram S, Smithies O, Maeda N. (1997). Hypertension, cardiac hypertrophy, and sudden death in mice lacking natriuretic peptide receptor A. *Proc Natl Acad Sci USA*. **94:** 14730-14735.

Oliver P, John S, Purdy K, Kim R, Maeda N, Goy M, Smithies O. (1998). Natriuretic peptide receptor 1 expression influences blood pressures of mice in a dose dependent manner. *Proc Natl Acad Sci USA*. **95:** 2547-2551.

Omori K & Kotera J. (2007). Overview of PDEs and their regulation. *Circ Res.* **100:** 309-327.

Ono K & Trautwein W. (1991). Potentiation by cyclic GMP of beta-adrenergic effect on Ca^{2+}current in guinea-pig ventricular cells. *J Physiol.* **443:** 387-404.

Onody A, Zvara A, Hackler L, Vigh L, Ferdinandy P, Puskas L. (2003). Effect of classic preconditioning on the gene expression pattern of rat hearts: a DNA microarray study. *FEBS Lett.* **536:** 35-40.

Opatowsky Y, Chen C, Campbell K, Hirsch J. (2004). Structural analysis of the voltage dependent calcium channel β subunit functional core and its complex with the α_1 interaction domain. *Neuron*. **42:**387–399.

Pagano M & Anand-Srivastava M. (2001). Cytoplasmic domain of natriuretic peptide receptor C constitutes G_i activator sequences that inhibit adenylyl cyclase activity. *J Biol Chem.* **276:** 22064-22070.

Perrin M & Gollob M. (2012). The role of atrial natriuretic peptide in modulating cardiac electrophysiology. *Heart Rhythm*. **9:**610-615.

Peterson B, DeMaria C, Adelman J, Yue D. (1999). Calmodulin is the Ca^{2+} sensor for Ca^{2+}inactivation of L-type calcium channels. *Neuron.* **22:**549–558

Pierkes M, Gambaryan S, Bokník P, Lohmann S, Schmitz W, Potthast R, Holtwick R, Kuhn M. (2002). Increased effects of C-type natriuretic peptide on cardiac ventricular contractility and relaxation in guanylyl cyclase A-deficient mice. *Cardiovasc Res.* **53:** 852-861.

Porter J, Arfsten A, Fuller F, Miller J, Gregory L, Lewicki J. (1990). Isolation and functional expression of the human atrial natriuretic peptide clearance receptor cDNA. *Biochem Biophys Res Commun.* **171:** 796-803.

Potter L & Garbers D. (1992). Dephosphorylation of the guanylyl cyclase-A receptor causes desensitization. *J Biol Chem.* **267:** 14531-14534.

Potter L & Garbers D. (1994). Protein kinase C-dependent desensitization of the atrial natriuretic peptide receptor is mediated by dephosphorylation. *J Biol Chem.* **269:** 14636-14642.

Potter L & Hunter T. (2001). Guanylyl cyclase-linked natriuretic peptide receptors: structure and regulation. *J Biol Chem* **276:** 6057-6060.

Potter L, Abbey-Hosch S, Dickey D. (2006). Natriuretic peptides, their receptors, and cyclic guanosine monophosphate-dependent signalling functions. *Endocr Rev.* **27:** 47-72.

Potter L. (2011). Natriuretic Peptide Metabolism, Clearance and Degradation. *FEBS J.* **278:**1808-1817.

Potthast R & Potter L. (2005). Phosphorylation-dependent regulation of the guanylyl cyclase-linked natriuretic peptide receptors. *Peptides.* **26:** 1001-1008.

Pragnell M, De Waard M, Mori Y, Tanabe T, Snutch T, Campbell K. (1994). Calcium channel β subunit binds to a conserved motif in the I–II cytoplasmic linker of the α_1-subunit. *Nature.* **368:**67–70.

Qu Y, Baroudi G, Yue Y, El-Sherif N, Boutjdir M. (2004). Localization and modulation of α_{1D} ($Ca_v1.3$) L-type Ca channel by protein kinase A. *American Journal of Physiology*. **288:** 2123-2130.

Rae J, Cooper K, GGates P, Watsky M. (1991). Low access resistance perforated patch recordings using amphotericin B. *J Neurosci Methods*. **37:** 15-26.

Rahmutula D, Nakayama T, Soma M, Kosuge K, Aoi N, Izumi Y, Kanmatsuse K, Ozawa Y. (2002). Structure and polymorphisms of the human natriuretic peptide receptor C gene. *Endocrine.* **17:**85–90.

Roberts, J, Davies R, Lubitz S, Thibodeau I, Nery P, Birnie D, Benjamin E, Lemery R, Ellinor P, Gollob M. (2010). Evaluation of non-synonymous *NPPA* single nucleotide polymorphisms in atrial fibrillation. *Europace*. **12:** 1078-1083.

Ren X, Xu C, Zhan C, Yang Y, Shi L, Wang F, Wang C, Xia Y, Yang B, Wu G, Wang P, Li X, Wang D, Xiong X, Liu J, Liu Y, Liu M, Liu J, Tu X, Wang Q. (2010). Identification of NPPA variants associated with atrial fibrillation in the Chinese GeneID population. *Clin Chim Acta*. **411:** 481-485.

Richards A, McDonald D, Fitzpatrick M, Nicholls M, Espiner E, Ikram H, Jans S, Grant S, Yandle T. (1988). Atrial natriuretic hormone has biological effects in man at physiological plasma concentrations. J Clin Endocrinol Metab. **67:**1134–1139.

Rose R, Lomax A, Giles W. (2003). Inhibition of L-type Ca^{2+} current by C-type natriuretic peptide in bullfrog atrial myocytes: an NPR-C-mediated effect. *Am J Physiol Heart Circ Physiol.* **285:** 2454-2462.

Rose R, Lomax A, Kondo C, Anand-Srivastava M, Giles W. (2004). Effects of C-type natriuretic peptide on ionic currents in mouse sinoatrial node: a role for the NPRC receptor. *Am J Physiol Heart Circ Physiol.* **286:** 1970-1977.

Rose R, Anand-Srivastava M, Giles W, Bains J. (2005). C-type natriuretic peptide inhibits L-type Ca2+ current in rat magnocellular neurosecretory cells by activating the NPR-C receptor. *J Neurophysiol.* **94:** 612-621.

Rose R, Kabir M, Backx P. (2007). Altered heart rate and sinoatrial node function in mice lacking the cAMP regulator phosphoinositide 3-kinase-gamma. *Circ Res.* **101:**1274 -1282.

Rose R & Giles W. (2008). Natriuretic peptide C receptor signalling in the heart and vasculature. *J Physiol.* **586:** 353-366.

Schoenfeld J, Sehl P, Quan C, Burnier J, Lowe D. (1994). Agonist selectivity for three species of natriuretic peptide receptor-A. *Molecular Pharmacology*. **47:**172-180.

Schotten U, Haase H, Frechen D, Greiser M, Stellbrink C, Vazquez-Jimenez J, Morano I, Allessie M, Hanrath P. (2003). The L-type Ca^{2+} -channel subunits α_{1C} and β_2 are not downregulated in atrial myocardium of patients with chronic atrial fibrillation. *J Mol Cell Cardiol.* **35:** 437–443.

Schweitz, H, Vigne P, Moinier D, Frelin C, Lazdunski M. (1992). A new member of the natriuretic peptide family is present in the venom of the green mamba (*Dendroaspis angusticeps*) *J Biol Chem*. **267:** 13928–13932.

Schulz-Knappe P, Forssmann K, Herbst F, Hock D, Pipkorn R, Forssmann W. (1988). Isolation and structural analysis of "urodilatin", a new peptide of the cardiodilatin-(ANP)-family, extracted from human urine. *Klin Wochenschr.* **66:** 752-759, 1988.

Schultz S, Singh S, Bellet R, Singh G, Tubb D, Chin H, Garbers D. (1989).The primary structure of a plasma membrane guanylate cyclase demonstrates diversity within this new receptor family. *Cell.* **58:** 1155-1162.

Senzaki H, Smith C, Juang G, Isoda T, Mayer S, Ohler A, Paolocci N, Tomaselli G,Hare J, Kass D. (2001). Cardiac phosphodiesterase 5 (cGMP-specific) modulates β-adrenergic signalling in vivo and is down-regulated in heart failure. *FASEB J.* **15:** 1718-1726.

Shaw, R & Colecraft H. (2013). L-type calcium channel targeting and local signalling in cardiac myocytes. *Cardiovascular Research.* **98:** 177-186.

Shima M, Seino Y, Torikai S, Imai M. (1988). Intrarenal localization of degradation of atrial natriuretic peptide in isolated glomeruli and cortical nephron segments. *Life Sci* **43:** 357-363.

Skanes A, Mandapati, R, Berefeld O, Davidenko J, Jalife J. (1998). Spatiotemporal periodicity during atrial fibrillation in the isolated sheep heart. *Circulation*. **98:** 1236-1248.

Smolenski A, Burkhardt A, Eigenthaler M, Butt E, Gambaryan S, Lohmann S, Walter U. (1998). Functional analysis of cGMP-dependent protein kinases I and II as mediators of NO/cGMP effects. *Naunyn Schmiedebergs Arch Pharmacol.* **358:**134-139.

Soderling S, Bayuga S, Beavo J. (1998). Cloning and characterization of a cAMP specific cyclic nucleotide phosphodiesterase. *Proc Natl Acad Sci USA.* **95:** 8991-8996.

Soderling S & Beavo J. (2000). Regulation of cAMP and cGMP signalling: new phosphodiesterases and new functions. *Curr Opin Cell Biol.* **12:** 174-179.

Sorbera L & Morad M. (1990). Atrionatriuretic peptide transforms cardiac sodium channels into calcium-conducting channels. *Heart Rhythm*. **9:** 610-615.

Soleilhac J, Lucas E, Beaumont A, Turcaud S, Michel J, Ficheux D, Fournié-Zaluski M, Roques B. (1992). A 94-kDa protein, identified as neutral endopeptidase-24.11, can inactivate atrial natriuretic peptide in the vascular endothelium. *Mol Pharmacol.* **41:** 609-614.

Splawski I, Timothy K, Sharpe L, Decher N, Kumar P, Bloise R, Napolitano C, Schwartz P, Joseph R, Condouris K, Tager-Flusberg H, Priori S, Sanguinetti M, Keating M. (2004). $Ca_v1.2$ calcium channel dysfunction causes a multisystem disorder including arrhythmia and autism. *Cell.* **119:**19–31.

Splawski I, Timothy KW, Decher N, Kumar P, Sachse FB, Beggs A, Sanguinetti, M, Keating M. (2005). Severe arrhythmia disorder caused by cardiac L-type calcium channel mutations. *Proc Natl Acad Sci USA*. **102:**8089–8096.

Springer J, Robbins C, Adamczyk A, McBoyle S, Bissell M, Rose R. (2012). The natriuretic peptides BNP and CNP increase heart rate and electrical conduction by stimulating ionic currents in the sinoatrial node and atrial myocardium following activation of guanylyl cyclase-linked natriuretic peptide receptors. *J Mol Cell Cardiol*. **52:** 1122-1134.

Steinhelper M, Cochrane K, Field L. (1990). Hypotension in transgenic mice expressing atrial natriuretic factor fusion genes. *Hypertension.* **16:** 301-307.

Stewart S, Hart C, Hole D, McMurray J. (2001). Population prevalence, incidence, and predictors of atrial fibrillation in the Renfrew/Paisley study. *Heart*. **86:**516–521.

Sudoh T, Kangawa K, Minamino N, Matsuo H. (1988). A new natriuretic peptide in porcine brain. *Nature.* **332:** 78-81.

Sudoh T, Minamino N, Kangawa K, Matsuo H. (1990). C-type natriuretic peptide (CNP): a new member of natriuretic peptide family identified in porcine brain. *Biochem Biophys Res Commun.* **168:** 863-870.

Suga S, Nakao K, Hosoda K, Mukoyama M, Ogawa Y, Shirakami G, Arai H, Saito Y, Kambayashi Y, Inouye K. (1992). Receptor selectivity of natriuretic peptide family, atrial natriuretic peptide, brain natriuretic peptide and C-type natriuretic peptide. *Endocrinology*. **130:** 229-239.

Sumii K & Sperelakis N. (1995). cGMP-dependent protein kinase regulation of the L-type Ca^{2+} current in rat ventricular myocytes. *Circulation Research.* **77:**803–812.

Swayze R & Braun A. (2001). A catalytically inactive mutant of type I cGMP-dependent protein kinase prevents enhancement of large conductance, calcium-sensitive K channels by sodium nitroprusside and cGMP. *J Biol Chem*. **276:**19729–19737.

Tajima M, Bartunek J, Weinberg E, Ito N, Lorel l. (1998). Atrial natriuretic peptide has different effects on contractility and intracellular PH in normal and hypertrophied myocytes from pressure-overloaded hearts. *Circulation.* **98:** 2760–2764

Takahashi Y, Nakayama T, Soma M, Izumi Y, Kanmatsuse K. (1998). Organization of the human natriuretic peptide receptor A gene. *Biochem Biophys Res Commun* **246:**736–739.

Takahashi N, Saito Y, Kuwahara K, Harada M, Kishimoto I, Ogawa Y, Kawakami R, Nakagawa Y, Nakanishi M, Nakao K. (2003). Angiotensin II-induced ventricular hypertrophy and extracellular signal-regulated kinase activation are suppressed in mice overexpressing brain natriuretic peptide in circulation. *Hypertens Res*. **26:**847–853.

Tamura N, Ogawa Y, Chusho H, Nakamura K, Nakao K, Suda M, Kasahara M, Hashimoto R, Katsuura G, Mukoyama M. (2000). Cardiac fibrosis in mice lacking brain natriuretic peptide. *Proc Natl Acad Sci USA*. **97:** 4239-4244.

Tohse N, Nakaya H, Takeda Y, Kanno M. (1995). Cyclic GMP-mediated inhibition of L-type Ca^{2+} channel activity by human natriuretic peptide in rabbit heart cells. *Br J Pharmacol.* **114:** 1076-1082.

Tsuruda T, Boerrigter G, Huntley B, Noser J, Cataliotti A, Costello-Boerrigter L, Chen H, Burnett J. (2002). Brain natriuretic Peptide is produced in cardiac fibroblasts and induces matrix metalloproteinases. *Circ Res.* **91:** 1127-1134.

Tsuneyoshi H, Nishina T, Nomoto T, Kanemitsu H, Kawakami R, Unimonh O, Nishimura K, Komeda M. (2004). Atrial natriuretic peptide helps prevent late remodeling after left ventricular aneurysm repair. *Circulation.* **110:**174 –179.

Vandecasteele G, Verde I, Rücker-Martin C, Donzeau-Gouge P, Fischmeister R. (2001). Cyclic GMP regulation of the L-type Ca^{2+} channel current in human atrial myocytes. *J Physiol.* **533:** 329-340.

Van Petegem F, Clark K, Chatelain F, Minor D. (2004). Structure of a complex between a voltage-gated calcium channel β-subunit and an α-subunit domain. *Nature.* **429:**671–675.

Van Wagoner, D, Pond A, Lamorgese M, Rossie S, McCarthy P, Nerbonne J. (1999). Atrial L-Ca^{2+} currents and human atrial fibrillation. *Circ Res*. **85:** 428-436.

Wahler G & Dollinger S. (1995). Nitric oxide donor SIN-1 inhibits mammalian cardiac calcium current through cGMP-dependent protein kinase. *American Journal of Physiology.* **37:**45–54.

Waithe D, Ferron L, Page K, Chaggar K, Dolphin A. (2011). Beta-subunits promote the expression of $Ca_v2.2$ channels by reducing their proteasomal degradation. *J Biol Chem.* **286:**9598–9611.

Wakili R, Voigt N, Kaab S, Dobrev D, Nattel S. (2011). Recent advances in the molecular pathophysiology and atrial fibrillation. *J Clin Invest*. **121:** 2955-2968.

Wang D, Oparil S, Feng J, Li P, Perry G, Chen L, Dai M, John S, Chen Y. (2003). Effects of pressure overload on extracellular matrix expression in the heart of the atrial natriuretic peptide-null mouse. *Hypertension.* **42:**88–95.

Wang H, George M, Kim J, Wang C, Pitt G. (2007). Ca_{2+}/calmodulin regulates trafficking of $Ca_v1.2$ Ca^{2+} channels in cultured hippocampal neurons. *J Neurosci* **27:**9086–9093.

Weber W, Fischli W, Hochuli E, Kupfer E, Weibel EK. (1991). Anantin—a peptide antagonist of the atrial natriuretic factor (ANF). I. Producing organism, fermentation, isolation and biological activity. *J Antibiot.* **44**:164–171.

Wijeyaratne C & Moult P. (1993). The effect of alpha human atrial natriuretic peptide on plasma volume and vascular permeability in normotensive subjects. *J Clin Endocrinol Metab.* **76:** 343-346.

Wit A & Boyden P. (2007). Triggered activity and atrial fibrillation. *Heart Rhythm*. **4:** 17-23.

Xiao R & Lakatta E. (1993). β1-adrenoceptor stimulation and β2-adrenoceptor stimulation differ in their effects on contraction, cytosolic Ca^{2+}, and Ca^{2+} current in single rat ventricular cells. *Circ Res.* **73:** 286-300.

Xu W & Lipscombe D. (2001). Neuronal $Ca_v1.3$ α_1 L-type channels activate at relatively hyperpolarized membrane potentials and are incompletely inhibited by dihydropyridines. *J Neurosci.* **21:** 5944-5951.

Yang-Feng T, Floyd-Smith G, Nemer M, Drouin J, Francke U. (1985). The pro-natriodilatin gene is located on the distal short arm of human chromosome 1 and on mouse chromosome 4. *Am J Hum Genet.* **37:** 1117-1128.

Yan W, Wu F, Morser J, Wu Q. (2000). Corin, a transmembrane cardiac serine protease, acts as a pro-atrial natriuretic peptide-converting enzyme. *Proc Natl Acad Sci USA.* **97:**8525-8529.

Yandle T, Richards A, Nicholls M, Cuneo R, Espiner E, Livesey J. (1986). Metabolic clearance rate and plasma half-life of alpha-human atrial natriuretic peptide in man. *Life Sci.* **38:**1827-1833.

Yang L, Katchman A, Morrow J, Doshi D, Marx S. (2001). Cardiac L-type calcium channel ($Ca_v1.2$) associates with gamma subunits. *FASEB J.* **25:**928–936.

Yue L, Feng J, Wang Z, Nattel S. (1999). Adrenergic control of the ultra-rapid delayed rectifier current in canine atrial myocytes. *J Physiol.* **516:** 385-398.

Zaccolo M & Movsesian M. (2007). cAMP and cGMP Signalling Cross-Talk: Role of Phosphodiesterases and Implications for Cardiac Pathophysiology. *Circ Res.* **100:** 1569-1578.

Zaccolo M. (2011). Spatial control of cAMP signalling in heath and disease. *Curr Opin Pharmacol*. **11:** 649-655.

Zhang M & Kass D. (2011). Phosphodiesterases and cardiac cGMP: evolving roles and controversies. *Trends Pharmacol Sci*. **32:** 360-365.

Zhang Q, Moalem J, Tse J, Scholz PM, Weiss H. (2005). Effects of natriuretic peptides on ventricular myocyte contraction and role of cyclic GMP signalling. *Eur J Pharmacol.* **510:** 209-215.

Zhang Z, He Y, Tuteja D, Xu D, Timofeyev V, Zhang Q, Glatter K, Xu Y, Shin H, Low R, Chiamvimonvat N. (2005). Functional Roles of $Ca_v1.3$ (α_{1D}) Calcium Channels in Atria Insights Gained From Gene-Targeted Null Mutant Mice. *Circulation.* **112:** 1936-1944.

Zuhlke R, Pitt G, Deisseroth K, Tsien R, Reuter H. (1999). Calmodulin supports both inactivation and facilitation of L-type calcium channels. *Nature.* **399:**159–162.